I give permission for public access to my thesis for any copying to be done at the discretion of the archives librarian and/or the College librarian.

_____ _____

Danelle Laflower Date

Measuring forest biomass using AIMS lidar and aerial high-resolution imagery

Danelle Laflower
Mount Holyoke College

Advisor:

Thomas Millette

A paper presented to the Faculty of Mount Holyoke College in partial fulfillment of the requirements for the Bachelor of Arts Degree

Department of Geology and Geography
Mount Holyoke College
South Hadley, MA 01075

May 2012

Contents

ABSTRACT

ACKNOWLEDGMENTS

INTRODUCTION 1

Biomass and carbon 2

Role of forests and ecological relevance of my research 2

Atmospheric carbon dioxide increases 3

Calculation of forest carbon 4

From empirical data 5

From remote sensing 7

Method limitations 11

AIMS system 11

Objectives 13

METHODS 14

Study area 14

Aerial site sampling parameters 15

Ground data sampling methodology 16

Transect level systematic sampling 16

Subplot level population data 20

Remote data 21

Stand height analysis 24

Height-DBH analysis 24

Estimating biomass 26
Biomass equations 26
Subplot-level ground measurements using actual DBH 27
Subplot-level remote estimates using lidar-estimated DBH and imagery 27
Spatial and statistical analysis 29
RESULTS 30
Spatial Autocorrelation 30
Stand Height 30
Preliminary analysis 30
Stand height significance 34
Height to DBH Regression 35
Subplot Biomass 38
DISCUSSION 43
Estimation of tree heights using lidar 43
Sampling design 43
Height analysis 44
Estimating DBH 45
Biomass 46
Biomass range and scaling 46
Within plot height variation 49
Red oak biomass consideration 50
Species identification 52
Stem density 53
Biomass comparison 55

RECOMMENDATIONS 60

CONCLUSION 62

APPENDICES 64

Appendix 1 64

Appendix 2 75

Appendix 3 76

Appendix 4 77

WORKS CITED 81

FIGURES

FIGURE 1. REPRESENTATION OF LIDAR DATA ACQUISITION PROCESS 9
FIGURE 2. LOCATION OF MOUNT HOLYOKE COLLEGE STUDY AREA. 15
FIGURE 3. FLIGHTLINES FOR REMOTE DATA ACQUISITION. 16
FIGURE 4. DOMINANT CANOPY TREES AND LIDAR LOCATION 20
FIGURE 5. SUBPLOT LOCATIONS AND LIDAR TRACE 21
FIGURE 6. MATLAB SCRIPT OUTPUT OF ELEVATION. 22
FIGURE 7. CORRECTED AND RAW GROUND LINES. 23
FIGURE 8A AND B. HEIGHT TO DBH REGRESSION 26
FIGURE 9A AND B. RESIDUAL PLOTS FOR HEIGHT TO DBH. 26
FIGURE 10. LIDAR AND GROUND PLOT HEIGHT HISTOGRAMS 31
FIGURE 11. DOT PLOTS OF INDIVIDUAL DATA POINTS IN EACH PLOT 32
FIGURE 12. SCATTERPLOT OF THE PLOT-LEVEL STANDARDIZED RESIDUALS. 32
FIGURE 13. LIDAR'S GENERAL UNDERPREDICTION 33
FIGURE 14. MEAN LIDAR HEIGHT REGRESSION 34
FIGURE 15. HISTOGRAMS OF DBH MEASUREMENTS 36
FIGURE 16. HEIGHT-TO-LN(DBH) SCATTERPLOTS OF COMMON SPECIES 37
FIGURE 17. SUBPLOT HISTOGRAMS OF GROUND AND LIDAR BIOMASS DATA 39
FIGURE 18. SCATTERPLOT OF THE DOMINANT CANOPY BIOMASS 39
FIGURE 19. REMOTE BIOMASS RESIDUALS FOR DOMINANT CANOPY 40
FIGURE 20. SCATTERPLOT OF TOTAL GROUND BIOMASS 40
FIGURE 21. REMOTE BIOMASS RESIDUALS FOR TOTAL BIOMASS 41
FIGURE 22. SAMPLING SCHEME GRID PATTERN OVER TREE CANOPY 44
FIGURE 23. RELATIVE PLOT HEIGHT 50
FIGURE 24. COMPARISON OF PERCENTAGE OF RED OAKS 51
FIGURE 25. RED OAK CANOPY COVER AND RED OAK BIOMASS. 52
FIGURE 26A AND B. NATURAL COLOR AND STANDARD DEVIATION STRETCH 54
FIGURE 27. OVER-ESTIMATION OF DOMINANT CANOPY TREES. 55
FIGURE 28. BIOMASS PER HECTARE ADJUSTED TO REFLECT ACTUAL VALUES. 59

Tables

TABLE 1. HEIGHT TO NATURAL LOG (DBH) REGRESSION EQUATIONS 37
TABLE 2. COMPARISON OF BIOMASS CALCULATIONS 42
TABLE 3. BIOMASS UNDERESTIMATION DUE TO LOWERED AVERAGE HEIGHT. 50
TABLE 4. RED OAK TREE COUNT COMPARISON FOR PLOT 388 57
TABLE 5. TOTAL TREE COUNT COMPARISON FOR PLOT 428 58

ABSTRACT

Increasing atmospheric carbon dioxide (CO_2) levels are a leading cause of climate change (Malhi et al. 2002). At least half of the Earth's terrestrial carbon is stored in forest biomass (Gower et al. 1996) by the photosynthetic conversion of atmospheric CO_2. Therefore, estimating forest carbon stocks helps us quantify carbon concentrations and potential sources and sinks for CO_2. One way that ecologists calculate biomass is with empirical allometric equations that use species and diameter at breast height (DBH) and divide by two to estimate carbon (Brown and Schroeder 1999, Jenkins et al. 2004).

I hypothesized that I could estimate stand-level biomass using the Airborne Imaging Multispectral Sensor's (AIMS) high-resolution imagery and lidar height measurements. To test this notion, I selected a study area on Mount Holyoke College property, in South Hadley, Massachusetts and systematically sampled 366 trees for species, height, DBH, and canopy data. I obtained lidar-derived canopy height and high resolution imagery with the AIMS system. For the ground validation of biomass, I created ten 900m^2 subplots, where I identified species, measured DBH for all live stems >12.4cm, and recorded place in the canopy. I calculated biomass using the corresponding biomass equations, summed the results, and scaled to hectare. I also calculated biomass using only dominant and co-dominant trees.

I averaged the lidar values and the ground-sampled trees' heights within each plot to obtain plot average height for each method. By dividing the area into 20 plots, a linear regression indicated that the lidar average height was a significant predictor of dominant ground-sampled tree average height ($p<0.001$, $R^2=0.658$).

To remotely estimate biomass, I identified species and stem density in georeferenced AIMS images of each subplot. From ground data, I created linear regression models to estimate DBH from height. I used lidar height to estimate DBH values in the species-specific allometric biomass equations found in Jenkins et al. (2004). I multiplied these biomass values by the number of stems of each species in the plot, scaled the value to hectare, and summed the results. I compared these results with the ground biomass data. The linear regression indicated that the remote method was a significant predictor of dominant tree ground biomass ($p=0.022$, $R^2=0.499$). These results suggest that this technique has the potential to adequately predict stand-level biomass in a southern New England forest. The next step will be to expand the dataset to determine the robustness of the method.

ACKNOWLEDGMENTS

I present this paper with deep appreciation to my advisor, Thomas Millette, who encouraged and supported my efforts to conduct this research and disseminate these results. I also owe a debt of gratitude to Eugenio Marcano, who has helped me obtain many skills, and supported me with tea and cookies. When I am stuck in a future GIS problem, I will ask myself, what would Eugenio do?

Thanks to Martha Hoopes for being on my committee and providing the critical review that I wanted. Thanks to Janice Gifford and Yue Zhao for their statistical assistance, and to Janice for also being part of my committee.

I want to thank Linnea Johnson for her good nature and ambition in collecting the 2010 data. It was a pleasure to spend a summer with her. Many people helped me collect additional data and I am grateful to them; Josh Laflower, Paul Laflower, Marshall Laflower, Dana Rubin, Skylar Supranaut, Erica Moody, Erin Frick, Gabriel Marcano, David Marcano, and Dean Gamache.

I also want to thank Caitlin Dickinson for sharing her experience regarding biomass calculations, and her and the UMass MIRSL lab for providing the Harvard Forest data to me.

I thank all of you who work in the GPL for being there. You all (and the windows) help to create a positive environment. Finally, to my friends and family, thanks for your support and patience through this endeavor.

INTRODUCTION

The world's forests are dynamic ecosystems that store 861±66Pg of carbon, according to some estimates (Pan et al. 2011). In addition to the uncertainty by 66 billion metric tons, the sizes and conditions of forested areas are continually changing. This suggests that the storage capacity of forests is also in constant flux. As the largest terrestrial carbon storage receptacle, decreasing forest stores are a factor in increasing atmospheric carbon dioxide levels (CO_2) (Malhi et al. 2002). Conversely, maintaining and increasing the sequestration capacity of the Earth's forests help slow the rate of atmospheric CO_2 increase. Because forests are important in biogeochemical cycling, researchers attempt to quantify this stored carbon. Since the only way to measure aboveground forest carbon accurately is to destroy the tree, it is necessary to find feasible, non-destructive methods to estimate terrestrial carbon stocks. My research examines a method of estimating biomass using profiling lidar to estimate average forest height, coupled with high-resolution imagery to determine forest composition.

Biomass and carbon

Approximately half of a tree's biomass (living or biological material of an organism) consists of carbon (Birdsey 1992, R. Houghton 2005) obtained by fixing atmospheric carbon dioxide (CO_2) during photosynthesis (H_2O+energy+ $CO_2 \leftrightarrow CH_2O+O_2$). The carbon accumulates as living and dead biomass in the environment, and animals, plants, and decomposing bacteria release the fixed carbon as CO_2, during respiration (Berg 2008).

Role of forests and ecological relevance of my research

Some researchers estimate that at least half of the Earth's terrestrial carbon is stored in forests (Gower et al. 1996), which currently cover approximately 30% of the Earth's surface (FAO 2010). The growing world population and increasing development are intensifying the pressure to shift land use from forest to urban or cropland. Taken together, global forest conversion and destruction are the second largest source of increased atmospheric carbon dioxide, from the release of stored carbon through respiration and combustion, and the loss of forests as a carbon storage reservoir (Schlesinger 1997, J. Houghton 2005, R. Houghton 2005).

Intact forests sequester carbon and generally contain more carbon than degraded forests and agricultural land (Malhi et al. 2002). Furthermore, selective harvesting may, and deforestation will, shift a forest from carbon sink to source. Because of the connection between forests and atmospheric CO_2, it is critical to quantify current carbon stocks as a basis for carbon accounting. In addition, the

quantification of carbon stocks is an essential part of documenting changes, measuring offsets, and pricing carbon emissions (McKinley et al. 2011). An improvement in our terrestrial carbon estimation abilities will facilitate the evaluation of carbon sequestration strategies and will better position us to respond to forest management practices and deforestation as participants in global climate change.

Atmospheric carbon dioxide increases

Since the advent of the industrial age, fossil fuel combustion and land use conversion from forests have been the predominant causes of increasing atmospheric CO_2 levels (Keeling 1973, IPCC 2007). Scientists expect that atmospheric carbon dioxide levels will continue to rise as a function of increasing worldwide fossil fuel consumption and rising populations (Archer 2005). Denman and colleagues (2007) state that although approximately 50% of an atmospheric CO_2 increase can be removed within 30 years, it will take a few hundred years to remove the next 30%, and thousands of years to remove the last 20%. Currently, CO_2 is the greenhouse gas with the largest effect on temperature, because of its relative abundance and atmospheric lifespan (Malhi et al. 2002). The increase in atmospheric CO_2 closely follows the increase in global average temperatures (J. Houghton 2005). Current climate data show that global average air and water temperatures have risen, sea level has increased, and northern hemisphere snow cover has decreased (IPCC 2007). Although change is

inevitable, the pace is such that many natural systems will not be able to adapt or evolve, and this will likely lead to decreased biodiversity and decreased native species populations (Hughes 2000, Groom et al. 2006). Species that have specific niches will adapt, move, or go extinct in response to the changing climate (Hughes 2000).

Calculation of forest carbon

The potential effects of climate change require substantial efforts to limit CO_2 emissions. At this time in history, much of the American public ignores the implications of a warming planet, and even concerned citizens continue consuming fossil fuels because alternatives are not readily available or are prohibitively expensive. Although there are efforts to transition from fossil fuel dependence, this process is slow and politically-charged. Because forests have the ability to sequester carbon, preventing deforestation, improving harvesting procedures, and restoring forests are practical, quantifiable mitigation strategies. Quantification includes calculating biomass, but because it is not possible or practical to directly measure every tree, ecologists have developed a number of surrogate methods.

From empirical data

The IPCC (2000) suggests that the preferred method to estimate forest biomass is through a dimensional analysis approach via the use of allometric equations. These are empirical, species-specific and generalized regression equations that calculate biomass based on a tree's diameter at breast height (DBH) (Brown and Schroeder 1999, Jenkins et al. 2004). This form of dimensional analysis relates the biomass of a tree to its DBH by use of empirical data (Whittaker and Woodwell 1967, Jenkins et al. 2003). Researchers obtain the species-specific algorithms by measuring the DBH, measuring the biomass via destructive sampling techniques, and then calculating the corresponding regression equations (Jenkins et al. 2003). These equations calculate biomass on a per-tree basis, and researchers determine plot-level biomass by either measuring every tree, or creating sample plots and scaling up (Jenkins et al. 2001). This field-based approach is time-consuming and expensive.

Most algorithms require only DBH because tree height is more difficult to measure in the field, leading to less available height data (Brown 2002). Earlier research also suggested that the addition of height did not improve the equations enough to warrant the extra effort (Brown 2002, Jenkins et al. 2003). Differences in growth rates due to environmental conditions suggest that researchers should use allometric equations from the same locality or region as the study site (Andersson et al. 2009). For this reason, the IPCC (2000) suggests testing the fit of biome-level equations by conducting a small direct measurement (destructive)

sampling of biomass for the area species. An additional limitation is an upward bias, or biomass overestimation, in large diameter trees, if the sample tree DBH measurements are larger than the DBH measurements used to create the equations (Jenkins et al. 2003). Because researchers expect the rate of biomass accumulation to decrease after a tree obtains some diameter, it is important for the equations to reflect all DBH measurements of the target trees (Jenkins et al. 2001).

Another common way to measure biomass is by expanding trunk-volume tree data (obtained from closed-canopy forests) with biomass expansion factors (BEF) (Brown and Schroeder 1999). The United States Department of Agriculture (USDA) Forest Service's Forest Inventory and Analysis (FIA) follow protocols to determine tree bole (trunk) volume by species. FIA provides data-generating volume tables where a user can input a set of tree metric data, choose output parameters such as volume equation and volume type, and receive estimated bole volume for their data (USDA 2010). A biomass expansion factor then scales tree bole volume to total aboveground biomass (Jenkins et al. 2001).

Both of these methods rely on empirical data. However, remote areas have a dearth of forest inventory information, and the inconsistency of methodologies limits large-scale biomass estimations (Boudreau et al. 2008).

From remote sensing

Because ground-based measurements are difficult and time-consuming, researchers also estimate biomass through modeling and by various remote sensing methods (Andersson et al. 2009, Tang et al. 2010). Remote sensing sensor systems have varying resolutions and can operate from satellites or airplanes. Generally, instruments operated from satellites have coarser resolution than those operated from airborne platforms (Andersson et al. 2009). Active sensors supply their own illumination sources and passive sensors measure reflected solar radiation (Andersson et al. 2009).

Andersson et al. (2009) describe two basic approaches to using remotely gathered data. The first approach is by classifying land cover and estimating biomass from known properties. This method is dependent upon the resolution of the raw images and known biomass estimations for the particular land cover classes. The second approach inputs remotely-gathered, forest variable information such as leaf area index (LAI), canopy height and shape, and/or tree part measurements, such as DBH, into allometric equations (Andersson et al. 2009). I am using the second approach by predicting DBH from lidar-derived canopy height and inputting the variable into the appropriate biomass equations.

Studies show lidar (light detection and ranging) to be an effective measurement device (Lefsky et al. 2002, Nelson et al. 2003, Popescu et al. 2004, Patenaude et al. 2004, Popescu 2007). Lidar uses lasers to measure distance by recording the amount of time that elapses between transmission and reception of a

laser pulse. A transmitter sends a pulse, which strikes an object and reflects back to a receiver (Fig. 1). There are two types of lidar projections, profiling and scanning. Profiling lidar is unidirectional, and the transmitter emits pulses in a single, fixed direction, whereas scanning lidar collects data points across a transect, as well as along it. The scan pattern provides data for a canopy surface model and the ability to define parameters such as height, crown diameter, and stand density (Popescu et al. 2011). In addition to scanning ability, lidar technologies vary from discrete return to full waveform. Full waveform lidar records the intensity of the laser pulse as a function of time, whereas discrete lidar records peaks in intensity (Harding et al. 2000). Discrete lidar measures one or more of these peak returns for each pulse. An additional characterization of a lidar system is its footprint, or diameter of the pulse on the ground, which is a function of distance from the lidar transmitter to the target object. Airborne, small footprint (~1.0m) scanning lidar can be very accurate for determining elevation ranges and vegetation heights (Zhao et al. 2011) although it is generally restricted to small-scale or regional areas because of associated costs. Preliminary research using large footprint (~64m), full waveform,scanning, satellite lidar shows promise in estimating vegetation parameters at both small and large scales (Popescu et al. 2011).

Scanning lidar provides a wider swath of data than profiling lidar, and full waveform lidar relays more information than discrete lidar. In general, the initial expenses, processing costs, and yearly maintenance for both scanning lidar and

full waveform systems are considerably higher than for a discrete return profiling lidar system (Thomas Millette, personal communication, June 2010).

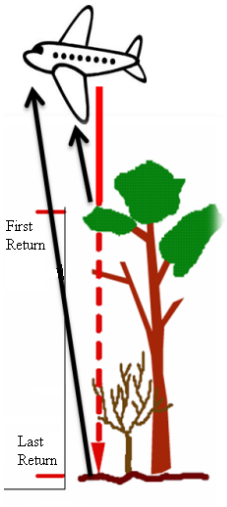

Figure 1. Representation of lidar data acquisition process. Image adapted from Harding (2000).

Popescu et al. (2004) used first and last return scanning lidar to estimate plot-level biomass in Virginia, USA. They developed linear regression equations to relate the lidar-derived canopy parameters with the field-based data and biomass estimates obtained using the generalized Jenkins et al. (2003) biomass equations for pines(R^2=0.82 and mixed hardwoods (R^2=0.39). Popescu (2007) also conducted a study in Texas, USA, to determine the feasibility of using dual return scanning lidar to estimate biomass at the individual tree level for loblolly pines (*Pinus taeda*). This survey used scanning lidar to estimate DBH through a lidar-derived height relationship and calculate biomass from known algorithms. This survey also estimated the biomass through direct non-linear regression of

lidar height and crown diameter measurements. In this study, the researcher was able to match 28% of the ground-measured trees with the trees visible in the lidar canopy-surface model. The lidar data from these 43 matched trees were used to predict field-measured DBH (R^2=0.87), and the lidar-derived DBH measurements were used to predict field-measured biomass (R^2=0.88). Lefsky et al. (2002) obtained promising results with a single model, using full waveform scanning lidar to estimate biomass in three temperate forest biomes (R^2=0.84). Nelson et al. (2003) obtained biomass estimates, using profiling lidar, that were within 20% of FIA database estimates in Delaware, USA.

Method limitations

All biomass estimation methods have limitations. Local direct measurement inventories lack broad scale spatial analysis without scaling and associated errors (Tang et al. 2010). Satellite technologies provide broad-scale information, but the resolution is usually coarse and may induce error at regional or smaller scales (R. Houghton 2005). Tang et al. (2010) consider that most large-scale models are too coarse for accurate regional accounting. Airborne scanning lidar systems and processing are expensive and generally suited for local or regional usage (Popescu et al. 2004, Boudreau et al. 2008), and airborne profiling systems can only measure a narrow strip along the transect. Therefore, climate scientists and others are researching many different types of technologies for this purpose, and it is likely that different technologies will be suited to different situations.

AIMS system

The technology that I am testing, the Airborne Imaging Multispectral Sensor (AIMS), provides fine spatial resolution data using an airplane platform, and includes an active sensor, profiling lidar, and a passive sensor, the natural color camera. The Mount Holyoke College Geoprocessing Laboratory (GPL) developed AIMS as a method for obtaining stand-level forest metrics to use for forest management or research (Millette and Hayward 2005). This technology uses a specially modified computer to integrate sub-meter precision GPS location

data and airplane orientation with lidar height measurements and high-resolution imagery. The system's profiling lidar component measures immediate distance of the aircraft from the ground and intermediate objects. The lidar component transmits low-intensity, near-infrared (905nm) laser pulses at 240Hz and measures the amount of time it takes for the reflected pulse to return to the receiver [(speed of light*time)/2=distance]. It measures the first and last return of each pulse, so that if the pulse hits a soft target, like the tree canopy, part of the pulse reflects back to the sensor (first return) and part of the pulse continues deeper into the canopy or to the ground before being reflected back (last return) (NCFMP 2003). A Trimble Ag 132, 12-channel differential GPS receiver with Omnistar satellite link is capable of locating the exact position of the airplane to sub-meter accuracy at 1.0Hz (Millette and Haward 2005). The attitude heading reference system (AHRS) records the orientation of the airplane (pitch φ, roll ω, yaw κ) at 10-50Hz. The data collected by the GPS and AHRS, which show aircraft location coupled with its pointing angle, provide ground coordinates of the lidar pulses. A full explanation of the AIMS system is available in Millette and Hayward (2005).

The AIMS system is similar to the PALS technology Nelson et al. (2003) and Boudreau et al. (2008) used to estimate biomass, although PALS has no mechanism for correcting for airplane orientation and uses video imagery in place of still images. The objective of Nelson and colleagues' (2003) methodology was to develop biomass regression equations from forest height and canopy density,

for various landcover classes, and compare their biomass values with those reported in the FIA databases. Their estimates were less than 20% different from the USDA Forest Service's Forest Inventory and Analysis (FIA) estimates.

Objectives

I looked for a significant relationship between tree height and DBH, so that I would be able to use lidar-derived stand height measurements to estimate DBH. I could then use the lidar-derived DBH values in conjunction with imagery-derived stand density and species ratios to estimate biomass using published equations. Such a method should offer biomass estimates more cheaply and rapidly than ground-sampling measurements. Since my remote methodology measures trees in the dominant canopy, I expected that the lidar would be able to predict average canopy height due to spatial autocorrelation (Zhang et al. 2003). I anticipated that the AIMS profiling lidar height averages would be effective, for estimating height, DBH, and hence biomass, at the right sampling density, in spite of the narrow (~1.0m wide) trace. My research is unique in that I am identifying species from aerial imagery so that I am able to estimate biomass with species-specific allometric equations. Because I also conducted a ground-sampled field study of the target area, I can compare my lidar-derived biomass estimates to ground-measured biomass.

METHODS

Study area

The study area is located on Mount Holyoke College property, in Massachusetts, on the South Hadley-Granby line (72º 30’ W: 42º 16’ N) (Fig. 2). Undeveloped land surrounds the area, except on the western edge, where it abuts the Orchards Golf Course. This area is located in the Connecticut River Valley ecoregion (US EPA 2012). Swain and Kearsley (2001) characterize the region, which receives approximately 100cm of precipitation annually, as having fertile soils, a mild climate, and rolling hills. In my study area, the elevation ranges from about 80-140m above mean sea level (USGS 1979), and the soils are generally fine sandy loams on 3-15% slopes, with the largest proportion being a Charlton fine sandy loam on 8-15% slopes (MAGIS 2010). The forest varies from predominantly conifer to predominantly deciduous on a west-to-east gradient. Red and white pines are the most abundant conifers. The red pine stand has the appearance of being a single-aged plantation, with little or no regeneration. The deciduous forest is central hardwood forest type (oak-hickory) (MFLA no date), and, like most of the northeast, the forest is second growth because of widespread deforestation in the 1800-1900s (Foster et al. 1998).

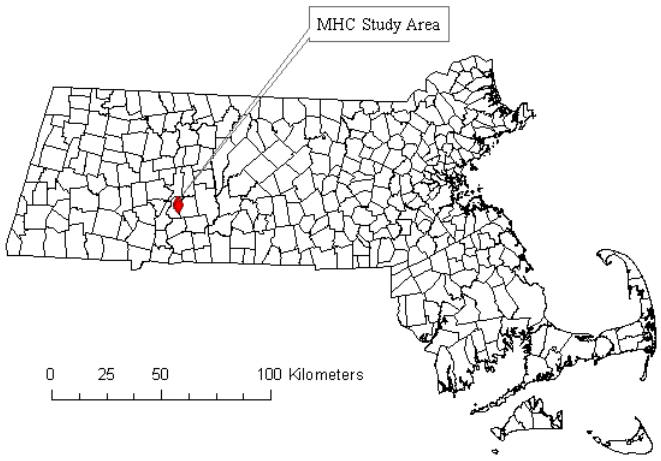

Figure 2. Location of Mount Holyoke College (MHC) study area.

Aerial site sampling parameters

In the summer of 2010 I participated in a summer research project to compare forest stand height using ground and remote sensing methods. For ground data collection we used geographic information system (GIS) software to create five 30m wide transects on the site that had conifer, deciduous, and mixed forest stands (Fig. 3). For aerial data collection, we created flightlines that were centered within the transects and oriented in a north-south direction. This led to an east-west flightline spacing of approximately 100-110m. Property boundaries and the Orchards Golf Course constrained the transect lengths, except for the short deciduous transect which was limited by time. The completed 30m wide transects cover approximately 10ha. On June 2, 2010, we flew the AIMS sensor, in a Cessna 172 airplane, over the flightlines, at an above ground elevation of

approximately 305m, to obtain georeferenced lidar height data and high-resolution color images.

Figure 3. Flightlines for remote data acquisition. We used each flightline as the center of each transect. The areas cover conifer (black and white lines), mixed (railroad symbol), and deciduous (solid lines) forest areas. The white line designates the Mount Holyoke property boundary.

Ground data sampling methodology

Transect level systematic sampling

Between May 26-July 12, 2010, we conducted a systematic sampling of trees in these transects using a 20m spacing in the north-south direction and a 10m spacing in the east-west direction. We sampled the closest live tree (with DBH >12.4cm) to each target location and identified species and recorded height, DBH,

and place in the canopy (dominant, co-dominant, intermediate, suppressed) for 344 trees. If I was uncertain of the species, I used the *Peterson Field Guide to Trees and Shrubs,* by George A. Petrides and *The Tree Identification Book,* by George W. D. Symonds. Because I had difficulty distinguishing red, black, scarlet, and pin oaks, I classified them by genus, as *Quercus* spp. I also classified the six sampled hickories to the genus, *Carya* spp., but identified all other trees at the species level. We used an Opti-Logic 1000LH hypsometer to determine tree heights. We measured the height of each sample tree three times if the results were within 1.0m, five times if the first three results were within 3m, and seven times if the variation in the first three measurements was greater than 3m. We also used a Suunto optical reading clinometer PM-5, occasionally as a height verification tool. We used a Forestry Suppliers Inc. 5m diameter tape to measure DBH at a height of 1.37m from the base of the high side of the tree. We nailed a uniquely numbered, 7cm x 2.54cm aluminum tree tag on the north side of each sample tree at a height of approximately 1.5m. In addition to sampling trees, we referenced their positions within the plots by beginning at one corner and taking distance and azimuth from one tree to the next using the transmitter and target of a Sonin Combo Pro electronic distance measurer (EDM) and a Suunto A-10 compass. To geographically locate each transect we collected coordinate data for one corner point, for 30 minutes, with a Trimble Juno ST GPS. We used GPS Pathfinder Office software (v. 4.10) to convert the GPS data into features and entered them into ArcGIS, a geographic information system (GIS) software. We

used GIS distance and azimuth tools to reference the sample trees to these features and joined our metric data (species, height, DBH, and place in canopy) as attributes.

I expanded this research independently in 2011 with the goal of estimating biomass. I supplemented the data by creating a new deciduous plot (using the sampling method previously described) and extending the mixed forest transect south by approximately 30m. This increased my total number of sample trees to 366. Since five transects are insufficient for a statistical analysis, I increased my sampling number by splitting the transects into smaller plots. To do this it was necessary to verify and/or improve the precision of the sample tree coordinates. I used a Trimble Pro XRS GPS and a 12m carbon fiber telescopic antenna, to get high enough into the tree canopy to get a carrier-phase satellite signal for the required 10 minutes. I obtained 27 sub-meter precision coordinate data points, in locations proximate to at least two- tagged sample trees. I took distance and azimuth from each GPS location to my sample trees and plotted both the GPS position data and the "new" sample tree locations in the GIS, where I used the spatial adjust editing tool to reference the original tree locations to the improved locations and update the coordinates of the sample tree data (Appendix 1).

When data are spatially autocorrelated, attributes are more similar between closer locations than further locations (Mitchell 2005). The variation in available resources within a forest creates a tendency toward spatial autocorrelation, although interspecies competition may also exhibit a negative spatial

autocorrelation where small trees neighbor large trees and vice versa (Zhang et al. 2003). However, we would not see this negative autocorrelation as the lidar only captures the height of the canopy trees. Since linear regression analysis assumes a random distribution, I split the transects into plots that were not spatially autocorrelated (Crone and Gehring 1997), by using the GIS to group lidar height data into four classes according to natural breaks in the data (Fig 4). I created plots that contained a predominance of a single height class data in an effort to avoid spatial autocorrelation between plots. This grouping method enabled me to create 20 variously-sized, non-spatially autocorrelated plots that included both lidar and sample tree data (Appendix 2). I excluded areas where the trees and the remote data did not coincide. Although the initial protocol was to measure the closest tree (DBH>12.4cm) to the target location, I filtered out suppressed and intermediate trees from plot-level height averages, since the lidar processing output calculates height by the tallest measurements. My height dataset contained 236 dominant and co-dominant samples (dominant canopy).

I classified the forest type of each plot with percent conifer. According to sample trees, plots with <33.33% conifer = deciduous, plots with 33.34-66.67% conifer = mixed, and plots with >66.68% conifer = coniferous plots. Although the original intent was to create an equal number of plots in each forest type, this methodology generated four conifer, twelve deciduous, and four mixed forest plots.

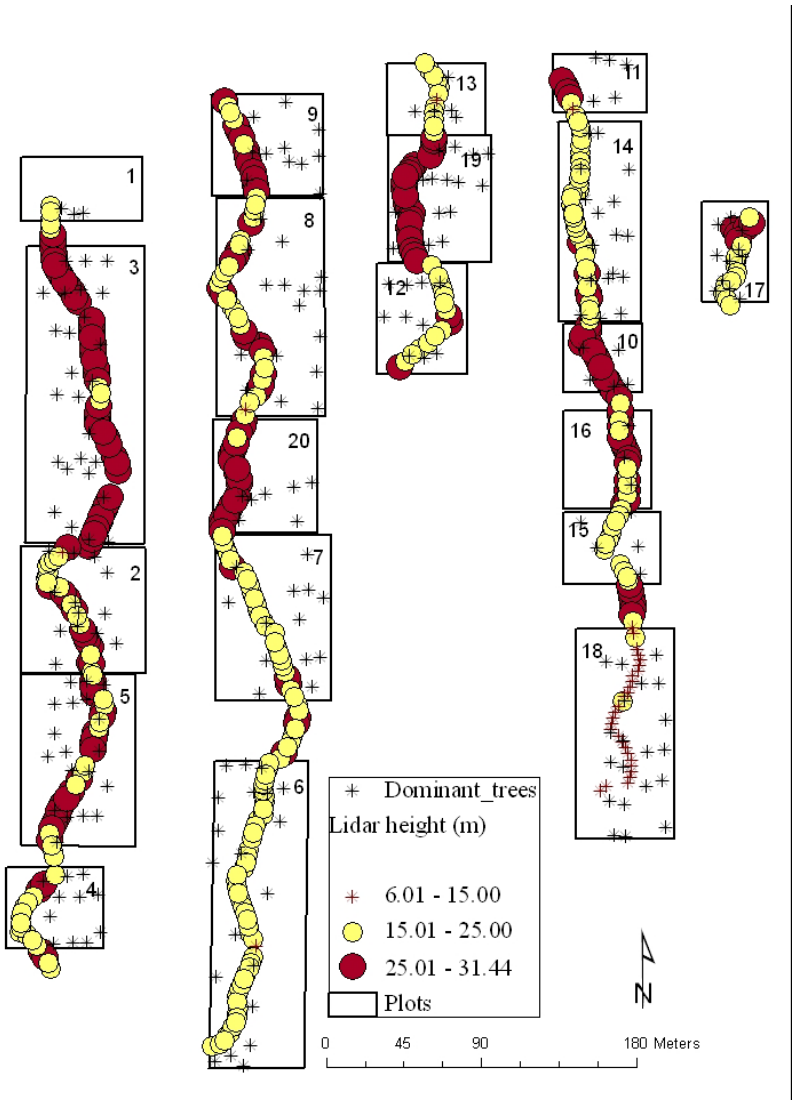

Figure 4. Dominant canopy trees and lidar location and heights in non-spatially autocorrelated plots.

Subplot level population data

I created ten 900m^2 subplots in mixed, conifer, and deciduous stands, on a varying stem density gradient, over the range of tree heights (Fig. 5). Within each plot, I counted all live stemmed trees, recorded species, place in canopy, and

measured DBH for all trees with a DBH >12.4cm. I scaled the results of the individual subplots to represent stem-density per hectare.

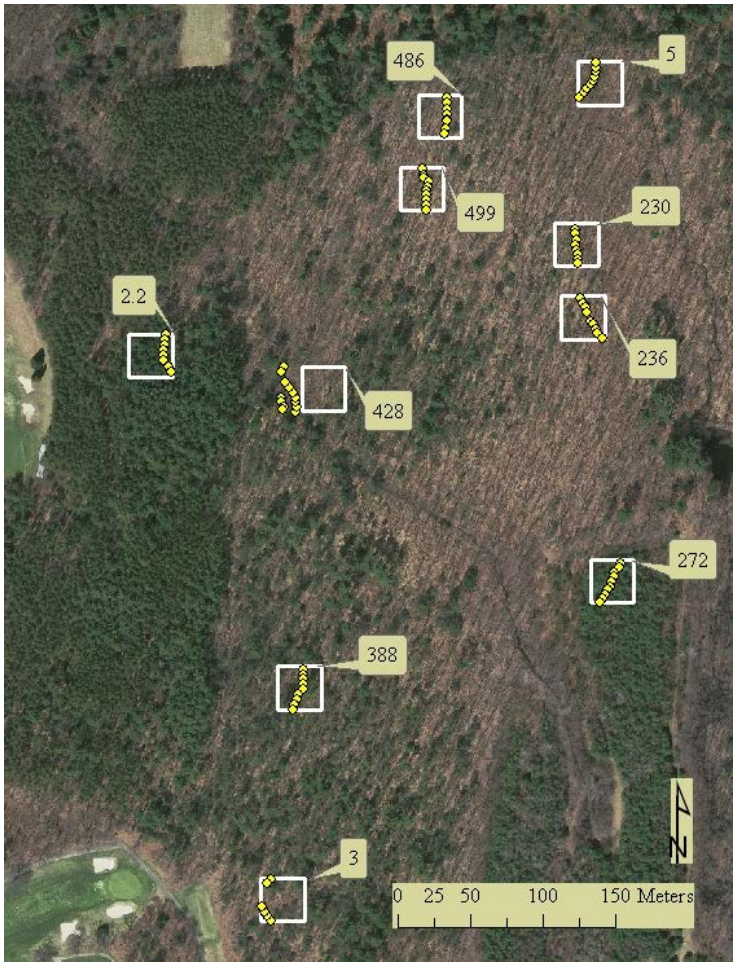

Figure 5. Labeled subplot locations and lidar trace (dotted yellow lines) on the corresponding MassGIS 2009 orthofoto. The orthophoto provides an indication of the forest type in each subplot.

Remote data

I processed the lidar and image data with GPL-developed software that matches the time of each measurement (GPS, AHRS, lidar, image) and created GIS layers of the lidar measurements' ground locations and the locations of the

centers of the images. I processed the lidar data with a MatLab script, also developed at the GPL. This program uses the first and last return lidar points to calculate ground line and canopy height by splitting the data into small time-segments and using the center value for the ground elevation and the minimum (the tallest point) for the canopy. I chose 0.1 second intervals to obtain the best canopy representation.

A careful analysis of the lidar data showed false ground lines in areas of dense forest canopy (Fig. 6). It was necessary to correct these ground lines to accurately assess this technology. In order to accomplish this, I compared the script output with a MassGIS, 5.0m digital elevation model (DEM) of the laser trace and corrected any false peaks, and then recalculated canopy height (Fig. 7).

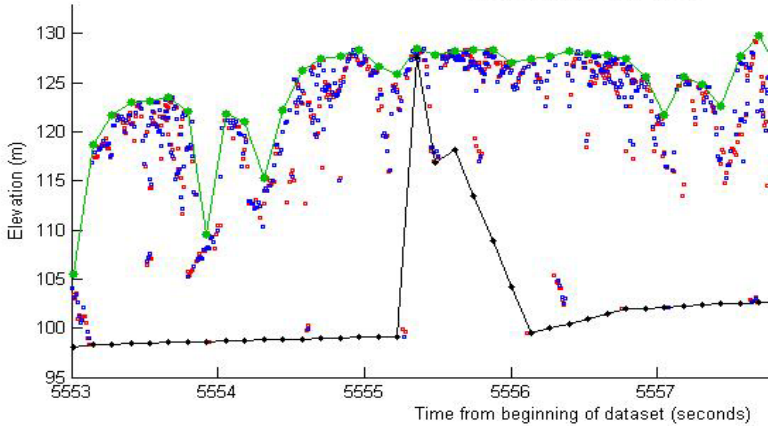

Figure 6. MatLab script output that shows a false change in elevation. The x axis is time in seconds and the y axis is elevation in meters. The points are lidar height data. The bottom line shows the estimated ground elevation and the top line shows the estimated canopy. The output shows a 25m ground elevation change because no lidar points were able to reach the ground within that sampling interval.

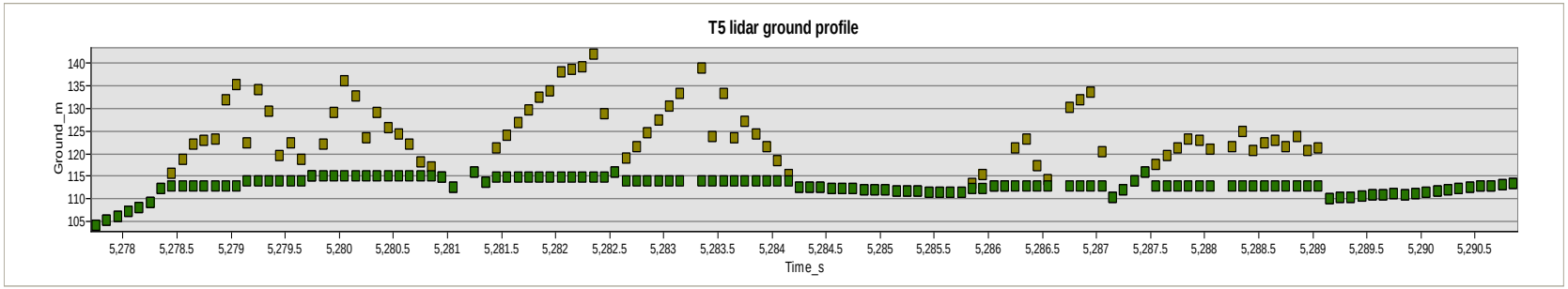

Figure 7. Corrected and raw ground lines. The x axis is distance from origin and the y axis is elevation. The corrected ground line is the smoothed line and the raw ground line has the series of false peaks.

Stand height analysis

To determine if I could substitute the lidar-derived plot average height for the ground-measured plot average height, I used GIS to obtain plot average heights for both the ground and lidar measurements using the 20 non-correlated plots.

I calculated a regression analysis to determine the relationship between measurement methods. To check for normality, I created histograms and a scatter plot of the residuals and created a series of dot plots to see how individual plot height measurements varied.

Height-DBH analysis

In order to be able to use the lidar-derived height measurement in the allometric biomass equations, I needed to be able to predict DBH from height. Previous researchers have documented species-specific relationships between a tree's height and its DBH (Denny and Siccama 2001, Sharma and Parton 2007). Therefore, I expected DBH and height to be related and created the set of height-to-ln(DBH) regression equations from my sample tree data. I separated the entire 366 tree dataset by species, created histograms and ran regression equations, using height to natural log(DBH) for red oak (*Quercus* spp.), white pine (*Pinus strobus*), black birch (*Betula lenta*), red maple (*Acer rubrum*), white oak (*Quercus alba*), red pine (*Pinus resinosa*), and hemlock (*Tsuga canadensis*). I used the natural log (ln) in order to have a linear relationship between height and DBH and

random variance in the residuals (Fig. 8a and b and Fig. 9a and b). I back-transformed ln(DBH) to DBH for input into the biomass equations. I pooled the other hardwoods, basswood (*Tilia americana*), beech (*Fagus grandifolia*), sugar maple (*Acer saccharum*), Norway maple (*Acer platanoides*), eastern cottonwood (*Populus deltoides*), big tooth aspen (*Populus grandidentata*), sassafras (*Sassafras albidum*), and white birch (*Betula papyrifera*) (<10% total), to obtain a generic "mixed hardwood" height-to-ln(DBH) regression equation. The five hemlocks I measured in my study area did not produce a significant regression model, therefore I supplemented the hemlock data by measuring height and DBH from nine additional hemlock trees in a mixed forested woodland in Wales, MA (72º 19' W: 42º 5' N).

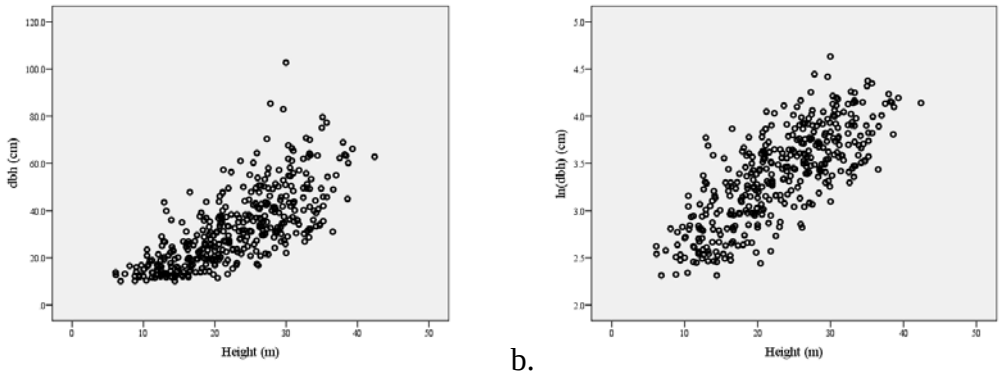

a. b.

Figure 8a and b. Height to DBH regression (on left) and height to natural log regression (on right). N=327.

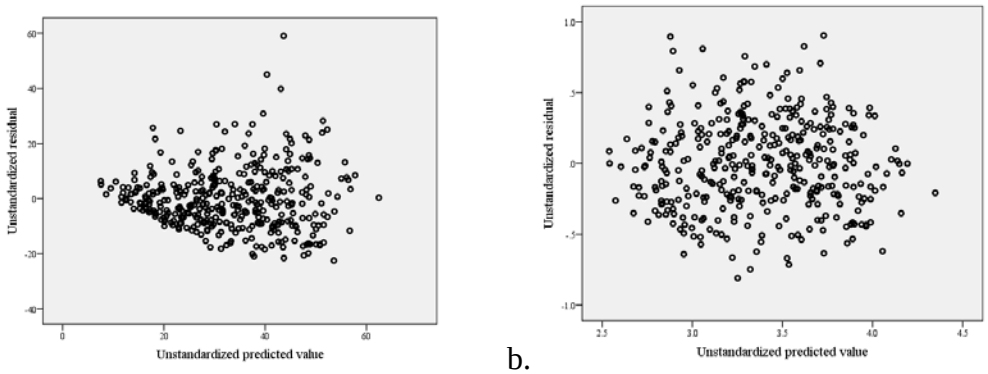

a. b.

Figure 9a and b. Residual plots for height to DBH (on left) and height to ln(DBH) (on right).

Estimating biomass

Biomass equations

For both ground and remote data, I used allometric equations found in Jenkins et al. (2004). These published equations predict oven-dry biomass of the entire aboveground portion of a tree. I chose the most appropriate species-specific equations that encompassed my sample trees' DBH (Appendix 3). I used the bigtooth maple (*Acer grandidentatum*) equation for the Norway maples

because both species have the same specific gravity and bark volume (Miles and Smith 2009). I also included the mixed hardwood regression equation found in Jenkins et al. (2003) for all deciduous species I could not identify in imagery (Appendix 3).

Subplot-level ground measurements using actual DBH

For each of the ten biomass plots, I input the DBH measurements (for all live stems >12.4cm DBH) into the appropriate species' biomass regression equations, summed the results, and scaled to hectare. I also completed this analysis using only dominant and co-dominant trees in each plot.

Subplot-level remote estimates using lidar-estimated DBH and imagery

In the GIS, I georeferenced the high-resolution images and delineated the biomass plots using identifiable, tagged-sample trees as locators (Appendix 2). I then used the high-resolution imagery to determine which species were present, their ratios, and the plot-level stem density. To determine the species, I used a photointerpretation key that Linnea Johnson ('13) and I developed in the fall of 2010. Our guide has color and texture comparisons for common species in the area. I also used Hershey and Befort (1995) and Sayn-Wittgenstein (1978) for additional information. I used a range of scales on the images, from 1:240 to 1:1000, to observe and compare color and texture of the trees. If I could not determine the species, I considered it a mixed hardwood and used the Jenkins et

al. (2003) equation for mixed hardwoods. I placed a color-coded mark (by species) on what I believed to be each tree. The identification of individual trees was clear-cut when adjacent trees were dissimilar species, or when there were spaces between the crowns. I also changed the image display to a standard deviation stretch to increase the variation in the crown coloration. For questionable trees, I relied on knowledge of a species' branching geometry and its minimum crown dimension at DBH > 12.4cm **(**Lamson 1987). Published DBH-to-crown relationships suggested minimum diameters of 6m for hardwood crowns, 3.5m for red pines, and 4m for white pines (Bonner 1964, Lamson 1987, Meyer 2011).

I input these data into a spreadsheet that scaled the number of trees per species to number per hectare, calculated the estimated DBH for the identified species from the plot-average lidar height, calculated biomass per tree per species, and then multiplied trees per species/ha by the biomass value to obtain biomass per hectare per species (Appendix 4). I summed the results of all species in the plot to obtain total biomass. To check for normality, I created histograms and a scatter plot of the residuals, and then conducted a regression using plot-level remote biomass as the independent variable and dominant tree ground biomass as the dependent variable.

The remote methodology (abbreviated as remote throughout the paper) consists of lidar-derived height averages, and species and stem density from images.

Spatial and statistical analysis

I used Microsoft Excel for all data entry and simple calculations, ESRI's ArcGIS Geospatial Analyst tool to determine spatial autocorrelation, ESRI's ArcGIS 10 for all GIS analysis except plotting tree locations, where I used the distance and azimuth tools in ESRI's Arcview 3.3. I used IBM's SPSS software for all other statistical analysis.

RESULTS

Spatial Autocorrelation

The 20-plot division along the four natural breaks in lidar height values produced average plots heights that were not significantly different from random, according to the spatial autocorrelation Moran's I tool in ArcGIS (z score=0.538, p=0.591). The results of the Moran's I analysis on the residuals also suggest that the residuals were not spatially autocorrelated (z-score=0.2035, p=0.8395).

Stand Height

Preliminary analysis

I conducted the formal analysis at the plot level, with one average height measurement, per plot, for each method (ground, lidar). However, I also looked at the overall height distributions. Here, the height data for both methods show a fairly normal distribution. The histogram of the lidar height data indicates a positive kurtosis, due to the abundance of lidar points in the 25m height range, and a left skew, due to the patch of young trees in plot 18 (Figs. 4 and 10). The wider spread of the ground data minimized the skew caused by the short plot, although it is visible (Fig. 10). Dot plots of data separated by plot show that height variation tends to be slightly larger in the ground data (Fig. 11).

At the plot-level, the residuals do not show a trend, and the outlier is due to the anomalous short plot (18) (Fig. 12). The x=y graph indicates the general trend for lidar to under-predict canopy height (Fig. 13). The differences between plot-average lidar height and plot-average ground height, varied from almost 9m shorter to 1.41m taller, although only two plots exhibited a positive difference.

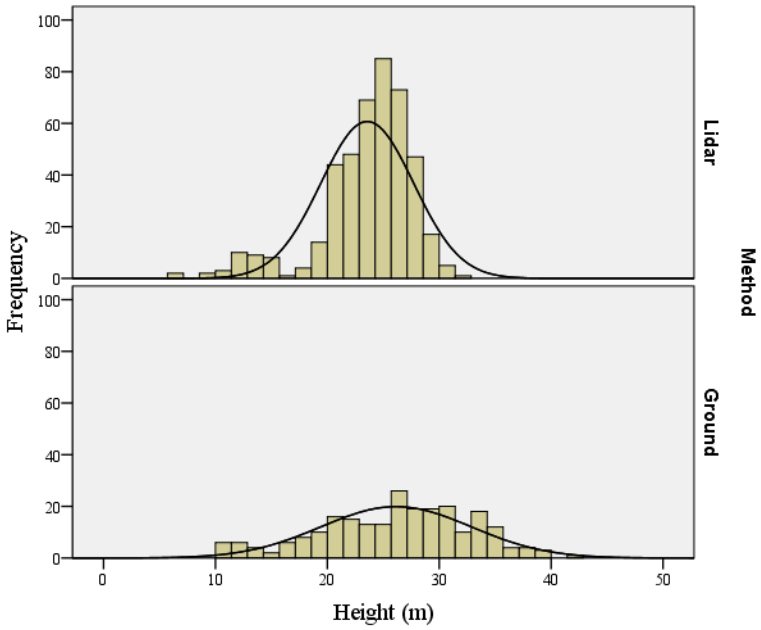

Figure 10. Histograms of lidar and ground plot height measurements. The solid lines represent a normal distribution. Ground mean 26.14m (s.d. 6.73 n=235). Lidar mean 23.56m (s.d. 4.15 n=442).

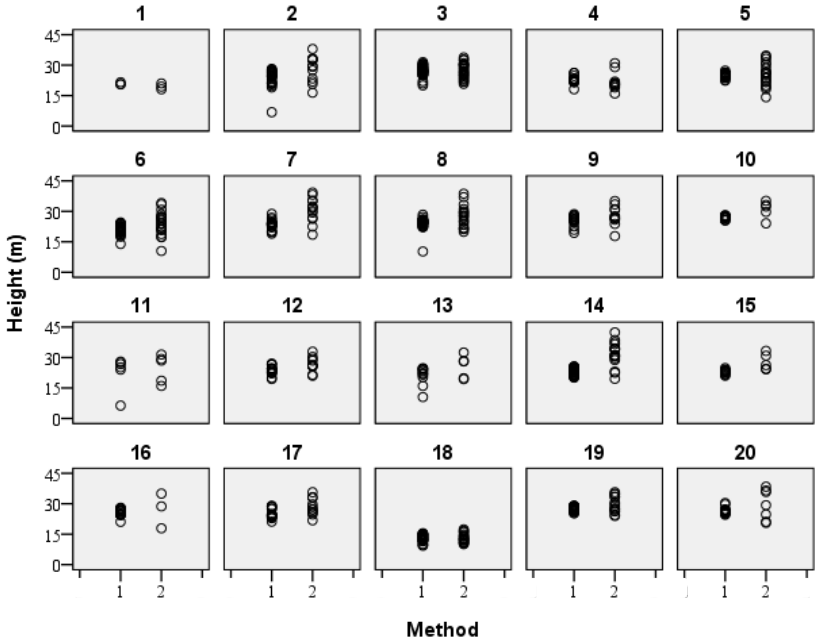

Figure 11. Dot plots of individual data points in each plot. 1=lidar 2=ground

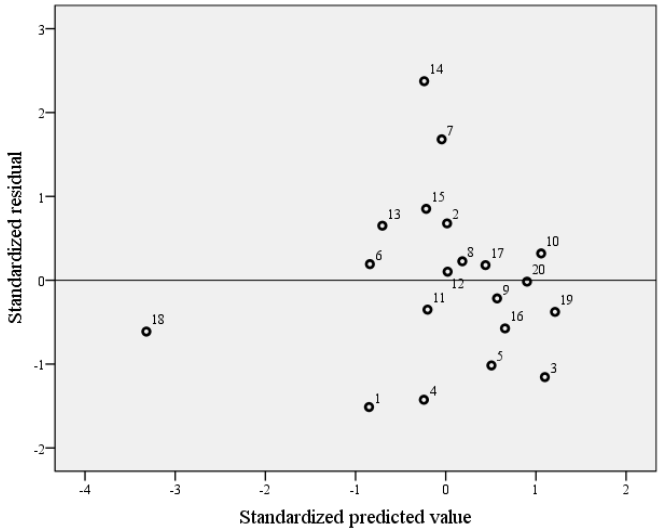

Figure 12. Scatterplot of the plot-level (labeled by plot number) standardized residuals.

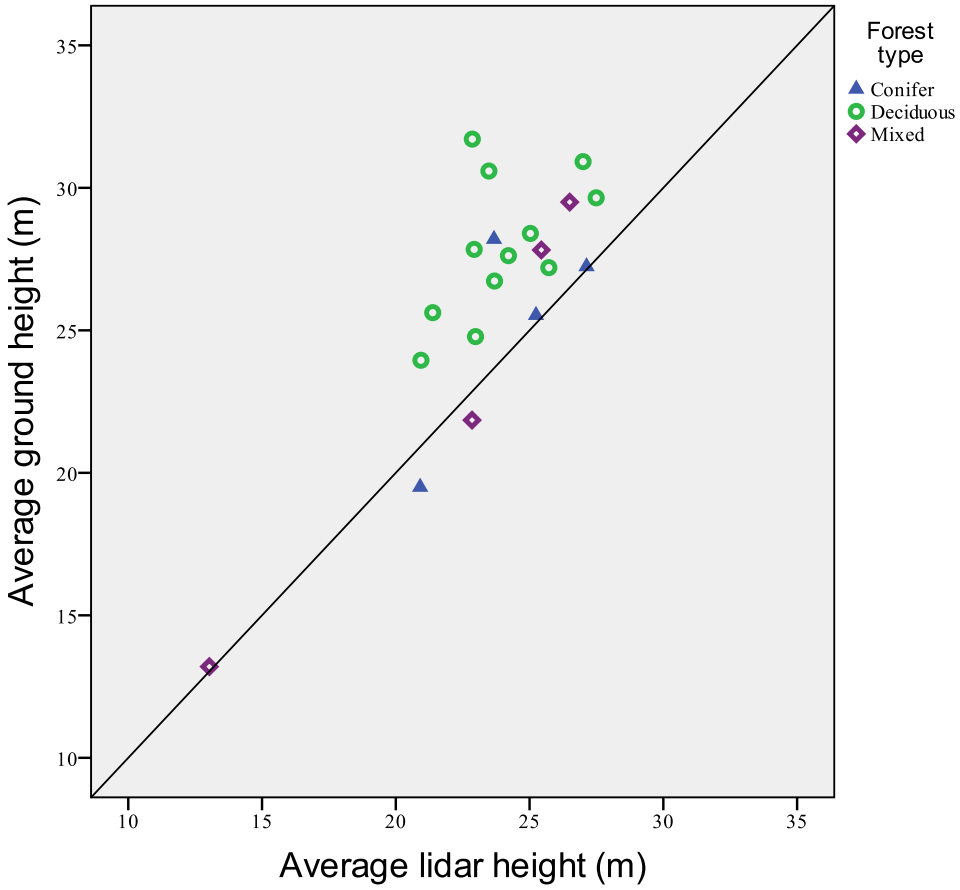

Figure 13. x=y line showing lidar's general underprediction when comparing ground-measured dominant and co-dominant tree plot height averages with the lidar plot height averages. Data points are labeled by plot number.

Stand height significance

Regression analysis using mean lidar plot height as the independent variable and mean ground plot height as the dependent variable yielded an R^2=0.658 with p<0.001 (Fig. 14). The positive constant and slope value >1 [y=0.511+(1.096*height)] indicate that lidar-derived height averages are shorter than ground-sampled height averages.

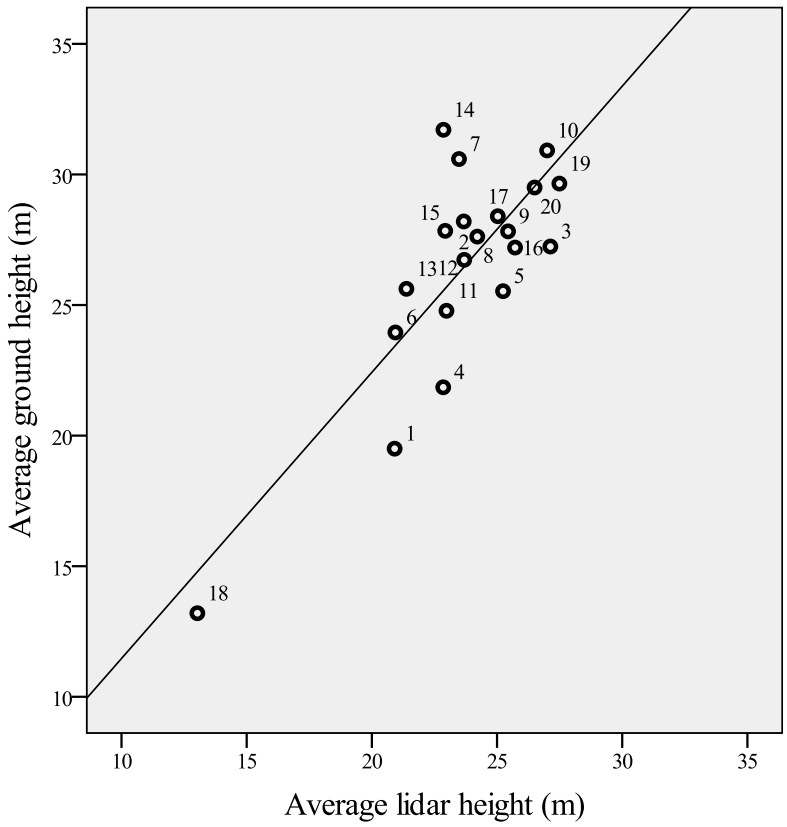

Figure 14. Regression line [y=0.511+(1.096*height)] using plot-level data with mean lidar height as the independent variable and mean ground height as the dependent variable.

Height to DBH Regression

Histograms of the DBH measurements for individual species indicated fairly normal distributions although the patch of young trees in plot 18 creates a bimodal distribution for white pine, and the presence of two large red maple trees widen the range for this species (Fig. 15). The scatterplot regression matrix illustrates the strength of the height-to-ln(DBH) relationships for the most common species in my study area (Fig. 16). The height-to-ln(DBH) regression equations show that height is a reasonable estimator of DBH for all of the species except red pine (Table 1). All of the equations are significant, but the red pine model does not explain the relationship between its height and its ln(DBH) (R^2=0.08), whereas the height-to-ln(DBH) models for the other measured conifers (hemlock and white pine) are more predictive. Although the red oak sample had 124 trees, the inherent variability that I found in the species' growth patterns precluded a strong R^2.

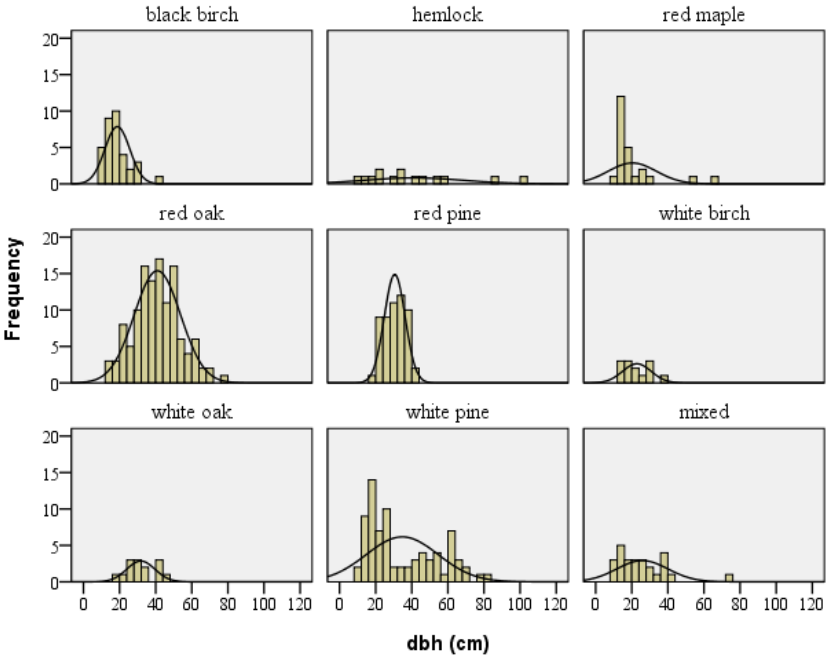

Figure 15. Histograms of DBH measurements for individual species and a mixed hardwood category.

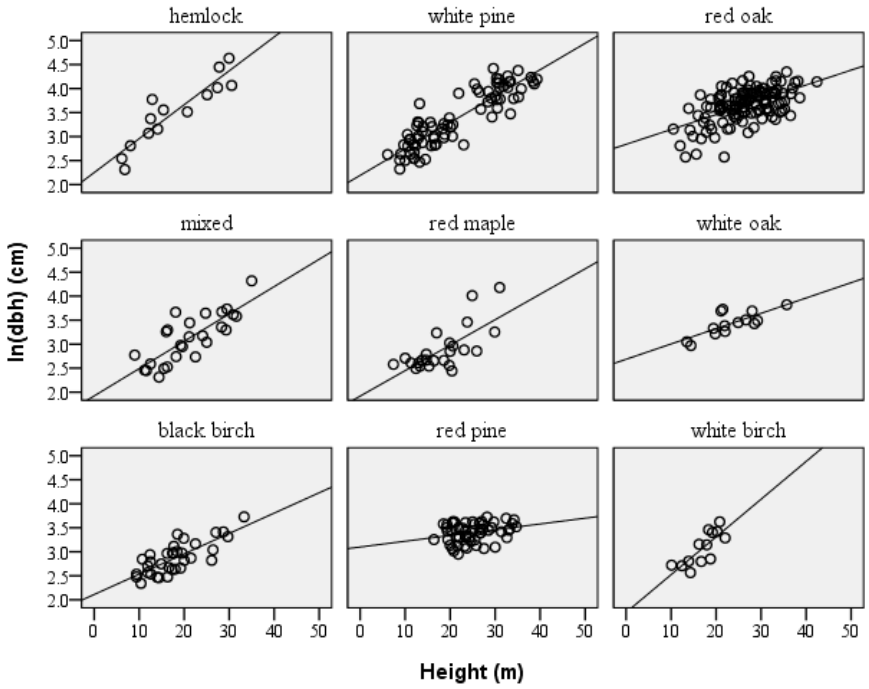

Figure 16. Height-to-ln(DBH) scatterplots of the most common species in the Mount Holyoke study area.

Table 1. Height to natural log (DBH) regression equations.
*significant ($p \geq 0.05$) **highly significant ($p \geq 0.01$)

Species	Ln(DBH) regression equation	R^2	sample size
Black birch	=2.11+(0.042*height)	0.60**	34
Red maple	=1.919+(0.053*height)	0.51**	24
White oak	=2.686+(0.032*height)	0.57**	14
Red oak	=2.839+(0.031*height)	0.32**	124
White pine	=2.192+(0.055*height)	0.79**	77
Red pine	=3.099+(.012*height)	0.08*	54
Mixed hardwood	=2.115+(0.049*height)	0.64**	26
Hemlock	=2.354+(0.064*height)	0.70**	10
Hickory spp	=1.8997+(0.0578*height)	0.81*	6
White birch	=1.7373+(.0786*height)	0.62*	13

Subplot Biomass

The plot level histograms highlight the difference in biomass distribution between both estimation methods (Fig. 17). With only 10 data points, it is difficult to get a sense of how the methods will compare on a larger scale. The regression analysis using the remote method biomass as predictor for the dominant canopy shows a significant regression for predicting the biomass of all dominant and co-dominant trees within a plot ($p=0.012$, $R^2=0.563$) (Fig. 18). The standardized residual scatterplot does not show any clear pattern (Fig. 19). Using the remote biomass estimation to predict total ground biomass was slightly less effective than for predicting dominant canopy biomass but still yielded a significant regression ($p=0.022$, $R^2=0.499$) (Fig. 20). The residuals do not seem to follow a pattern (Fig. 21).

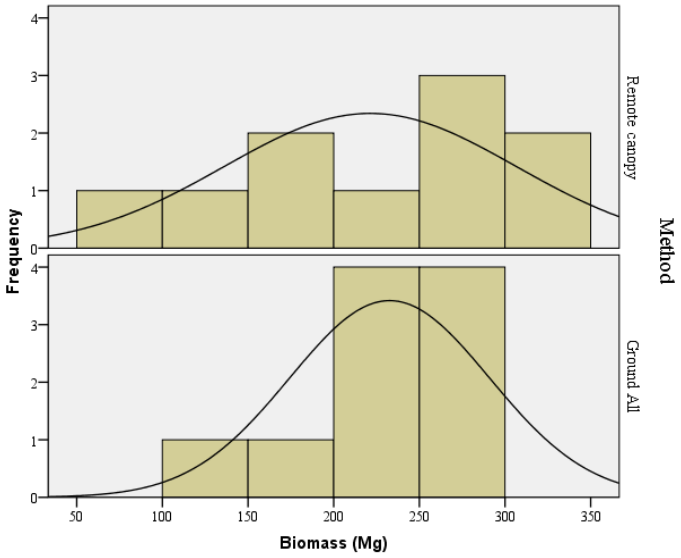

Figure 17. Histograms of ground and lidar biomass data for the 10 subplots scaled to the hectare level. The top histogram shows the remote method data distribution and the bottom histogram shows the total ground biomass data distribution.

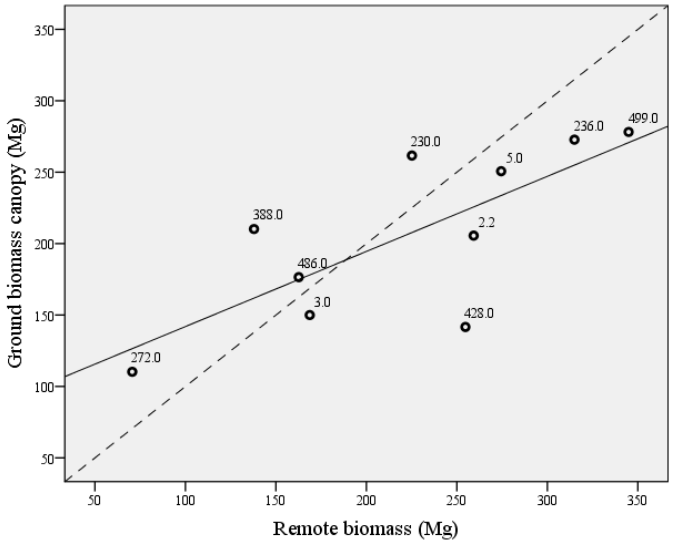

Figure 18. Scatterplot of the labeled plots for dominant canopy biomass using the remote method as the independent variable and the ground-measured biomass as the dependent variable. Ground dominant tree biomass in megagrams (Mg)=89.333+(0.526*remote biomass estimation(Mg)). Dashed line y=x.

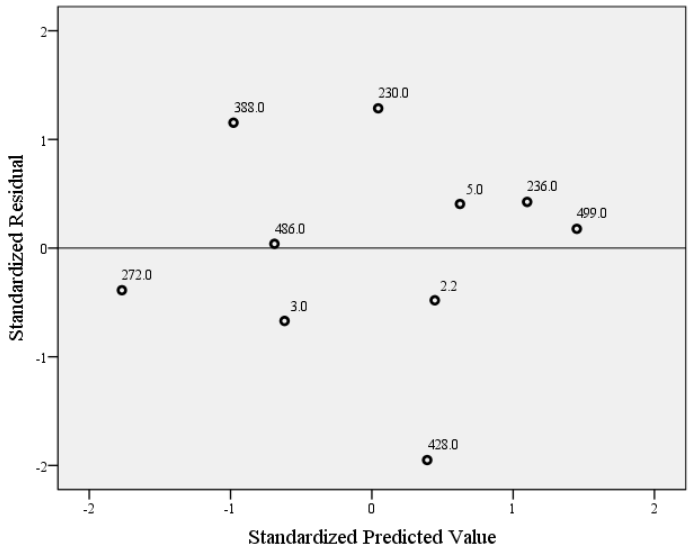

Figure 19. Scatterplot of the plot residuals of remote biomass as predictor of dominant canopy biomass. Standardized predicted values are on the x axis and the standardized residuals are on the y axis. All values are within two standard deviations.

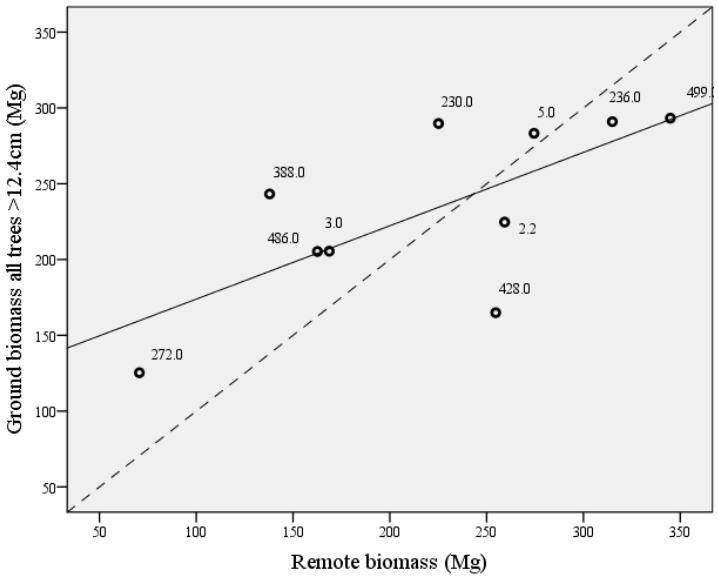

Figure 20. Scatterplot regressing total ground biomass against the remotely estimated biomass. Total ground biomass (for all trees with DBH>12.4cm) =125.492+(0.499*remote biomass estimation). Dashed line, y=x.

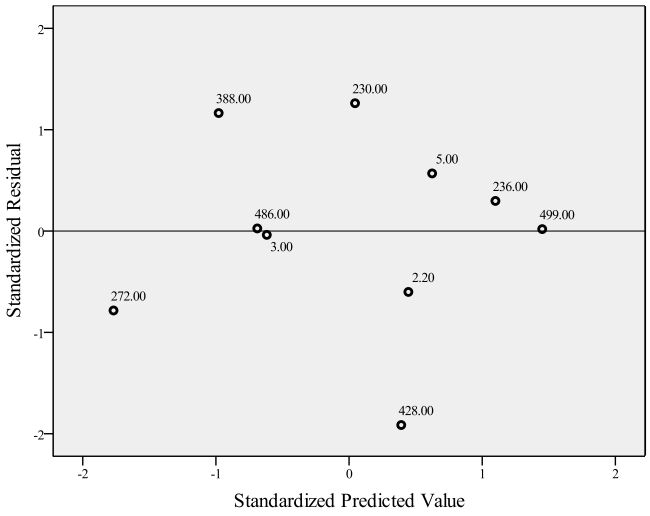

Figure 21. Scatterplot of the residuals of remote biomass as predictor of total biomass (all trees DBH>12.4cm). Standardized predicted values are on the x axis and the standardized residuals are on the y axis. All values are within two standard deviations.

Because the remote methodology only measures trees in the dominant canopy, I expected a general underestimation of biomass when comparing remotely-calculated biomass with total ground-measured biomass. This was not always the case, although there was more underestimation than overestimation (Fig. 20, Table 2).

Table 2. Comparison of remotely calculated biomass with ground biomass.

Plot	Remote biomass (Mg/ha)	Ground biomass all trees (Mg/ha)	Difference remote-ground (Mg/ha)	Remote error = Difference/ ground biomass	Lidar plot height average (m)
2.2	259.27	224.66	34.61	0.15	30.14
3	168.69	205.48	-36.79	-0.18	24.05
5	274.47	283.25	-8.78	-0.03	28.03
230	225.15	289.72	-64.57	-0.22	27.24
236	314.95	290.94	24.01	0.08	29.88
272	70.62	125.34	-54.72	-0.44	14.22
388	137.90	243.24	-105.34	-0.43	24.98
428	254.70	164.92	89.78	0.54	27.77
486	162.60	205.32	-42.72	-0.21	26.13
499	344.90	293.26	51.64	0.18	31.22
Sum	2213.25	2326.13	-112.88		

DISCUSSION

Estimation of tree heights using lidar

Sampling design

The initial expense of flying the AIMS system is considerable, so for profiling lidar to be a cost-effective technology, researchers need to obtain data over large areas. However, ground sampling is time-intensive, so foresters often estimate metrics by collecting population-level data as subplots within a sample area and scaling the results; or by conducting a systematic sampling of the target area (Avery and Burkhart 1993). We chose to conduct a systematic sampling, using a ground-sampling scheme that would allow us to obtain height data over long transects. Our 10m*20m rectangular grid pattern provided an adequate representation of the forest canopy for my study, although I would have obtained better ground representation if all of the trees I measured within the grid pattern were canopy trees (Fig. 22). After I removed the suppressed and intermediate trees, there were areas without adequate ground data. Where data were sparse but existent I retained the plot area; where it was nonexistent, I eliminated that area of the transect from the data (Fig. 4).

Figure 22. Sampling scheme (10*20m) grid pattern over ~20-30m tall tree canopy. Used to verify sampling density. Dominant canopy stem density ~240 trees/ha.

Height analysis

The regression analysis indicated that stand height averages were lower when using lidar measurements. The histograms and dot plots of the full data set corroborate the lower value with the lidar averages (Fig. 10 & 11). This under-prediction of canopy height agrees with published research (Patenaude et al. 2004) and may be a result of each laser pulse's penetration into the deciduous canopy before reaching enough vegetative mass to reflect a return pulse (Gaveau and Hill 2003). Nelson et al. (1997) cited earlier researchers who found that the

conical nature of conifers created a negative bias in lidar height measurements and that lidar tended to under-predict pine forest average canopy heights by 8-10%. My conifer plots show conflicting data with an over-prediction of 7% in plot 1, an under-prediction of nearly 20% in plot 2, and nearly equivalent values in plots 3 and 5. Plot 1 has very limited datapoints (3 lidar and 3 ground), and therefore cannot reliably be used as an indicator for over-prediction of height.

The significant results (R^2=0.658) of the regression model suggest that a profiling lidar trace can predict average forest stand height. However, the under-prediction meant that the regression model was necessary to convert the average lidar height values to the average ground height.

Estimating DBH

Allometric equations use DBH because it is easy to measure accurately, as opposed to height, which is much more difficult and time consuming to collect in the field. This particular analysis benefitted from my measurement of trees over a large DBH and height range (Appendix 1). Since I based my hypothesis on plot-level height and biomass values, the variation around the regression line seemed to be acceptable.

Results indicate a significant relationship between a tree's height and its DBH, for all of my measured species, except red pine (Fig. 16 and Table 1). Although red pine showed no quantifiable relationship between height and DBH, these specimens may have reached their maximum height (Sharma and Parton

2007) and continue grow in diameter according to their ability to capture resources. Since we need more research before using height to estimate red pine DBH, I chose subplots without red pine. Another consideration is the red oak regression, which is highly significant but has a fairly weak predictive capability. The R^2 improved when I ran a regression on the small subset of the red oaks that were single-stemmed trees from the forest interior. However, I chose to use the full dataset regression model because of its much larger sample size and the notion that the equation would produce a reasonable average DBH from height, with overestimations and underestimations balancing each other in the model. My data indicate a great deal of inherent variation in growth patterns within the species. It is possible that my consolidation of oaks (black, red, scarlet, pin), into a single category, contributed to the wide range in values.

As a final consideration, the effectiveness of these models may be limited to this study area because I did not take resource availability or stem density into consideration when creating these models (Sharma and Parton 2007).

Biomass

Biomass range and scaling

Ecologists have found that old growth is the type of forest that contains the largest values of aboveground biomass density (AGBD) (Brown et al. 1997). Brown and Schroder (1999) found that old-growth forests in the eastern United States had an average AGBD range of 220-260Mg/ha. They compared this to the

FIA database's values of 50-150Mg/ha and 75-175Mg/ha for conifer and hardwood forests, respectively (Brown et al. 1997). Since my study area is not an old growth forest, I expected the values to fall below those published by Brown and Schroder, but four of my ten biomass plots had scaled biomass values over 260Mg/ha, for both the ground and remote calculations (Table 2). However, Jenkins et al. (2001) cite research with published hardwood biomass values from 31.9-431Mg/ha. My data are well within this range. July 2009 data from 15 1.0ha plots in Harvard Forest, in central Massachusetts, have biomass values that range from 119-268Mg/ha (Cook et al. 2011). In addition to the direct calculation of biomass, Cook et al. (2011) also subdivided the 1.0ha plots into 16 subplots and calculated biomass in each, and then scaled to the hectare. These biomass data range from 51-515Mg/ha (with the scaling) over all of the subplots, with an overall average biomass of 140.68Mg/ha. This range indicates a high level of variability within and between the 1.0ha plots, but the overall average remains within FIA expectations. The variation introduced by the scaling should be noted because I obtained my results by scaling each 900m^2 plot to the hectare level [(10,000m^2/ha)/900m^2=11.1111]. Since a common measurement unit for forest biomass is Mg/ha, future research using this methodology should aim to estimate biomass in 1.0ha plots to avoid errors caused by scaling to the measurement level, as evidenced in the Cook et al. (2011) data. However, the forest variation ultimately must determine plot size. Although averages are useful parameters, it is the calculation of plot-level variation that will enable us to improve upon

current large-scale biomass estimates. For example, in my subplots, the average ground-data biomass is 232Mg/ha and the average remote-data biomass is 221Mg/ha. These very similar results mask plot-level variation and errors.

Within plot height variation

In addition to scaling-induced errors, future research must consider the within-plot lidar height variation. In one of my preliminary analyses, I divided the area into 1.0ha plots and used my remote methodology to estimate biomass. What I found was that one of the 1.0ha plots had both a mature, tall forest section and a young, short forest section (Fig. 23). Using the average height of the entire plot gave me a total estimated biomass value of 96.63Mg/ha, but separating the plot and calculating the two sections separately gave me a total estimated biomass value of 167.90 for the area (Table 3). I obtained a lower value in the full plot because height predicts DBH and the DBH increase-to-biomass increase for small trees is not linear (Jenkins et al. 2001); so the lower average height suppresses the overall plot-level biomass. Brown et al. (1997) found that a small proportion of large diameter trees (DBH>70cm) could comprise up to 30-40% of a forest's biomass. Depressing the height subsequently constricts the DBH and therefore the biomass. In order to use height to estimate biomass, researchers need to determine how much within-plot height variation can occur while maintaining effective estimations. This area is an example of forest variation that requires an alteration of the target 1.0ha plot size.

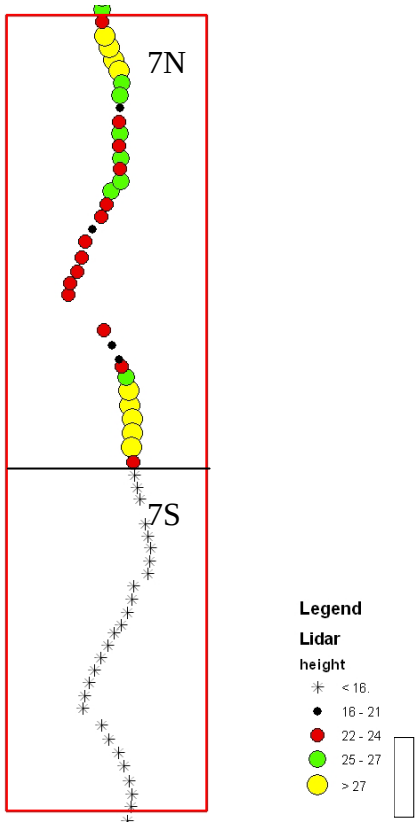

Figure 23. Lidar height values indicating relative plot height in meters. This 1.0ha plot (plot7) is 200m*50m.

Table 3. Biomass underestimation due to lowered average height.

Plot	Average lidar height (m)	Estimated biomass (Mg/0.5ha)	Estimated biomass (Mg/1.0ha)
7 N + S	19.49	na	96.63
7 N	25.77	103.11	206.22
7 S	14.74	64.79	129.59
Sum of 7N + 7S biomass		169.90	

Red oak biomass consideration

In addition to concerns about scaling and plot height variation, I noticed the large effect red oaks have on the total biomass. Published specific gravity

values indicate that red oak is among the densest species in this study area (Jenkins et al. 2003). I generally underestimated the number of canopy-height red oak in each deciduous plot (Fig. 24). When I could not positively identify a species, I used the mixed hardwood regression height to DBH regression and the generic mixed hardwood allometric biomass equation, which calculate a lower biomass value than the red oak equation. Additional photointerpretation experience should help to minimize the underestimation. I ran some analyses to determine the disproportionate influence red oaks have on biomass in these plots (Fig. 25). The contribution of red oaks to the total biomass was always larger than their proportion in the canopy. The density and abundance of this species highlight the importance of accurately identifying red oaks in the images.

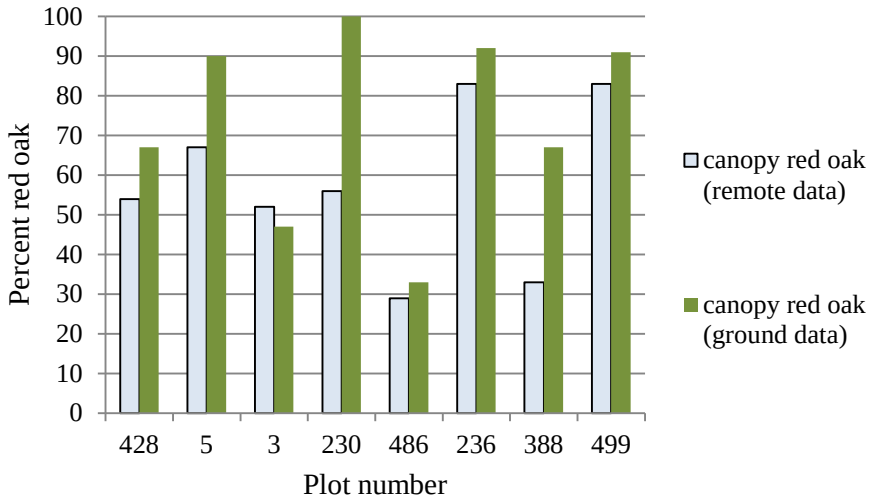

Figure 24. Comparison of percentage of red oaks I identified in the imagery with the percentage of red oak canopy trees in each plot.

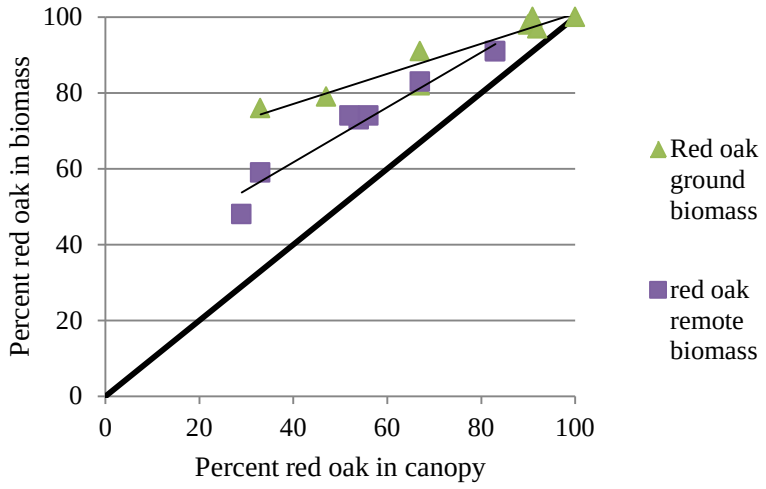

Figure 25. Relationship between red oak canopy cover and red oak biomass. Triangles are ground data and squares are remote data. The x=y line highlights the influence of red oak. The trendlines show the strength of these relationships. Red oak ground biomass=61.28+(0.3965*% canopy red oaks). Red oak lidar biomass= 32.692+(0.7253*% red oak identified).

Species identification

The final methodology consideration is the photointerpretation analysis, where I identified species and counted stems in the GIS. I found that it was crucial to have spent some time learning how to identify species in the high-resolution imagery and I believe that with some training examples and a good photointerpretation key, this method can produce satisfactory results. I frequently referred to the identification key and used ground-identified species that were locatable in the imagery for comparisons. It will be important for researchers to have some knowledge of potential forest species.

Stem density

To count individual trees, it was necessary to make them as distinct as possible. Switching from natural color to a standard deviation histogram stretch, in the GIS, enhanced the color variation and increased image contrast. This helped to delineate crowns (Figs. 26a and b). In order to determine individual trees in a two-dimensional image, it is necessary to be able to identify full and partial crowns. This is somewhat challenging because trees with segmented crowns can have the appearance of being multiple trees. Using minimum crown diameters helped me avoid some of the error, although large branches likely produced some misleading results. Although I expected that my minimum crown diameter criterion would underestimate what is visible in imagery due to the crown overlap that occurs in a natural forest stand, I generally over-counted stems (Fig. 27). This may be the result of seeing and counting trees that I classified as intermediate on the ground or more likely, of classifying dominant branches as trees. These results suggest that I introduced a level of inconsistency by counting trees with segmented crowns as multiple trees. The two plots where I under-estimated the dominant canopy had the highest overall stem densities and the highest proportions of conifers where it would have been more difficult to overestimate stem density. In addition, pines generally do not have multiple crowns and therefore researchers would be less likely to overestimate stem density.

Figure 26a and b. Natural color (top) and standard deviation stretch (bottom) of an area within my study site. The stretch is one technique to help distinguish individual trees.

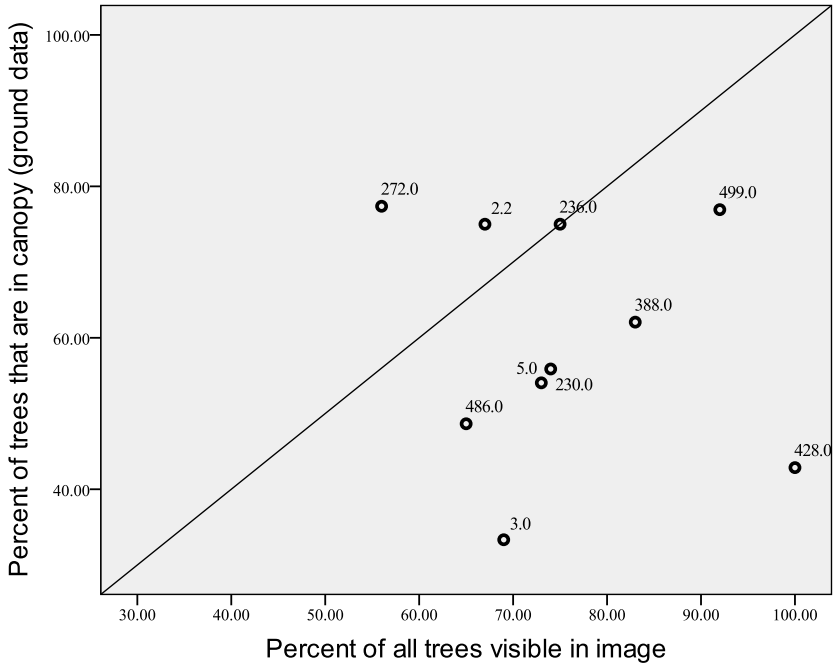

Figure 27. Scatterplot illustrating over-estimation of dominant canopy trees. [Percent of dominant canopy visible in image=(image stem density/actual ground stem density)*100] as the predictor for [percent of trees in the dominant canopy=(actual dominant canopy stem density/actual ground stem density)*100].

Biomass comparison

I chose sample plots that would encompass a range of forest types and ages. Neither the ground nor remote method histograms indicate a normal distribution, but this may simply be an effect of the small sample size (n). Even with the small n, the regression model (remote biomass as a predictor of total biomass) suggests that the remote method is a significant predictor of ground biomass, and the R^2 indicates that the model explains about half of the variation in calculation methods. Predicting dominant canopy biomass from the remote biomass improves the R^2 (0.562). This model has the advantage that I am

comparing the same data, the dominant canopy that is visible in the imagery. However, I do not focus on that regression, since the goal was to estimate total biomass.

We must use caution in analyzing these results because of the small sample size (10), but some of the sources of variation in the remote measurement are identifiable. I examined the three plots with a greater than 30% difference in biomass calculations (Table 3). Plot 272 seems to be a primary succession forest, with an average tree height of approximately 14m. This plot has a very high actual stem density of over 1500 trees/ha (1189 canopy trees), but I was only able to see 855 trees/ha in the image. Here the biomass underestimation is a direct result of the stem density underestimation. In plot 388, I underestimated the number of canopy-height red oaks and overestimated the number of mixed hardwoods, which underestimated the remote biomass values (Fig. 24). In a test analysis, where I substituted the number of red oaks and mixed hardwoods to reflect the actual stem count proportion while maintaining the lidar height data, I obtained biomass results that compared very favorably to the ground-measured data (Table 4). In plot 428 however, I also underestimated the percentage of canopy height red oaks, but in this plot, the remote estimation method overestimated the biomass. I counted the correct number of stems in the plot (28), but this is actually an overestimation, since I should have only been able to see ~12 canopy trees in the image, instead of 28, according to my ground data. To examine this relationship, I used a test similar to the proportion of red oak in plot

388, except that I scaled the total number of trees visible in the image to reflect what I should have seen, and again obtained very favorable results (Table 5). Possibly, the proportion of species types and relatively sparse nature of the plot allowed me to count the intermediate trees as well as the dominant trees in the image, which would affect the estimation, since I use one lidar height to obtain DBH measurements. Further experience determining stem density should minimize this source of error. One additional consideration for the biomass discrepancy in this plot is the location of the lidar points. Although the lidar trace does not pass directly over this plot, over half of the plot is within 25m of the lidar trace and there is no obvious difference in crown diameter or forest stage, so I expect that the lidar height source location is of small consequence (Fig. 5).

Table 4. Red oak tree count comparison for plot 388. Biomass is a function of average lidar plot height converted to DBH and input into the appropriate regression equation.

Original tree count as seen in images	Original remote biomass	Substituted tree count	Substituted biomass	Ground Biomass
8 red oaks	82Mg	16 red oaks	165Mg	
9 mixed hardwood	34Mg	1 mixed hardwood	4Mg	
Sum	139Mg		191Mg	210Mg

Table 5. Total tree count comparison for plot 428. Biomass is a function of average lidar plot height converted to DBH and input into the appropriate regression equation.

Original tree count =28 trees	Original remote biomass	Altered tree count =12 trees	Altered remote biomass	Ground Biomass
1 white pine	4Mg	1 white pine	4Mg	
3 black birch	14Mg	1 black birch	5Mg	
15 red oak	186Mg	9 red oak	112Mg	
3 red maple	16Mg	0 red maple	0	
6 mixed hardwood	34Mg	1 mixed hardwood	6Mg	
Sum	255Mg	Total altered	126Mg	165Mg

As the data show, the remote methodology may overestimate biomass (Table 3). I expect that improving the quantification of dense species such as red oak and consistently determining stem density would minimize the difference; but additional research would help to test this potential. Except for plot 5, the plots with the highest average heights are the ones that overestimate biomass (Table 2). There is also the possibility that the height regression model is not linear.

Furthermore, in my preliminary analysis, I conducted a backwards multiple regression using remote biomass, lidar height, and percentage red oak as the independent variables, and ground biomass as the dependent variable. The first variable excluded was remote biomass. This suggests that my methodology, in its current form, weakens the predictive power of lidar-derived heights to estimate biomass. Using only lidar plot average height as the predictor and ground biomass as the dependent variable yielded an R^2=0.54 with p=0.16. However, an improvement in the remote methodology results may change this

relationship. This is evident because even more favorable results occurred using lidar height and actual percent red oak (R^2=0.69, p=0.16). These analyses suggest that we may be able to obtain good results with height and red oak data or height data alone. We need to conduct more research to determine which variables are important and under what conditions.

My methodology is a series of estimations; I use lidar to estimate plot height, then use plot height to estimate each species' average DBH, then use the average DBH in the appropriate biomass equation, scale that biomass to the hectare level, and sum the results. Although each individual step introduces some level of error, I expect that we can minimize these errors by refining the methods (Figure 28). Currently, the mean error is less than 25% for plot level biomass (Table 2). Any improvements should make this a feasible method for estimating stand-level biomass.

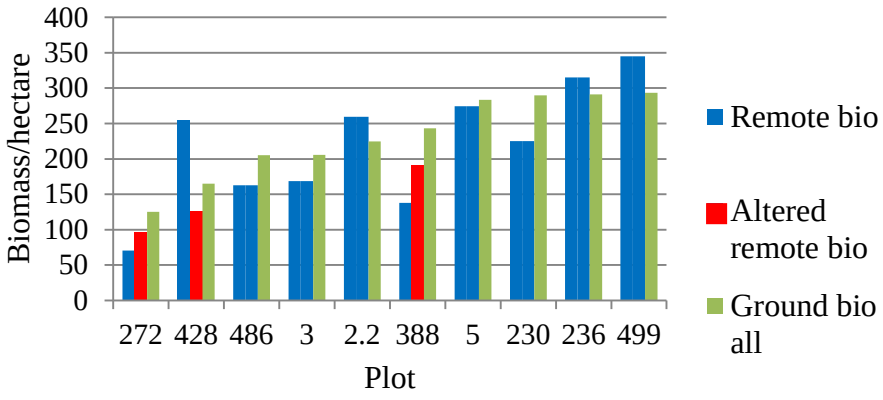

Figure 28. Biomass per hectare adjusted to reflect actual values for plots 272, 428, and 388. The red bars represent data that reflects actual stem density (plots 272, 428) or percent red oak (388). I did not alter the data for any of the other plots. These changes improve the predictive ability of the remote methodology (R^2=0.74).

RECOMMENDATIONS

My ground transects were an average of 30m wide, but for future studies comparing average stand height, I would increase the width to 50m in order to estimate average lidar height using 50m*200m, 1.0hectare plots, assuming normal homogeneity in the canopy. This sampling scheme, at 20m*10m density, obtains data for an average of 60 trees per hectare. In addition, I would establish a goal of two consecutive 100m long plots per area (30 trees per 50m*100m plot). This will provide the ability to determine average height at both the hectare and half-hectare level and enable researchers to determine the maximum effective plot length for obtaining average height measurements for use in estimating biomass. Because the goal is to obtain plot-average heights, researchers may need to increase the sampling density if the stem density is high, or the canopy height and crown diameter are highly variable.

The predicted canopy height from lidar regression model is sufficient for my study, but is too limited for use as a generic equation. Therefore, the next step is to conduct more research, over multiple areas, to create a robust regression equation so that further ground verification is not required. Since using ground measurements to obtain tree heights is time intensive, I recommend delineating plots with defined edges and at roadway borders, and obtaining the remote (lidar

and image) data before conducting any actual ground measurements to avoid measuring ground areas with no lidar data due to variation of the airplane path.

I also recommend creating a series of images as training exercises to improve red oak identification and stem density delineation. This should improve the biomass regression equation.

CONCLUSION

Having accurate forest height data is a key parameter for remote biomass estimation. This study adds to the collection of lidar research, and further documents the potential value of using remote sensing technologies to obtain forest metric data. My results suggest the possibility of using lidar for estimating forest stand height. I expect that further research, if conducted measuring only canopy height trees within the remotely sampled area, will show lidar to have a better predicting ability of average plot height than my results indicated. The methodology holds promise for estimating forest biomass; however, the ability to identify species and consistently count stems is crucial for accurate biomass estimation.

This study also provides a framework for designing future height and biomass estimation lidar studies. The stand height prediction results warrant additional research, with a goal of obtaining a useable (average lidar-to-average ground) regression equation for the northeastern United States.

Since the results of my small dataset show a significant relationship between ground- and remotely-measured plot biomass, it would be worthwhile to collect the additional data required to clarify both the potential applications and limitations of using lidar height and imagery to estimate biomass.

The benefit of using lidar and high-resolution imagery is its relative affordability and its adaptability. Although flight time is expensive, the flight to obtain my data took just over an hour and covered approximately 10 ha. These results suggests that my methodology, if developed, may allow scientists to obtain approximate biomass estimates in varied forest applications effectively and at a lower cost than with traditional ground-based and stereoscopic remote sensing methods.

APPENDICES

Appendix 1. Sample tree data for the Mount Holyoke Study Area. Canopy (1=dominant, 2=co-dominant, 3=intermediate, 4=suppressed). Forest type (<33.33% conifer = deciduous, plots with 33.34-66.67% conifer = mixed, and plots with >66.68% conifer = coniferous). Coordinates are Massachusetts State Plane Coordinate System, mainland NAD 1983. Plot and forest type data with NA are tree data that I excluded from the dataset because of lack of lidar data or because it was an intermediate or suppressed tree. I included these trees in this appendix since I used them in the height to dbh regression equations.

Tag #	Species	Canopy	Height (m)	DBH (cm)	Plot	Forest type	Easting (m)	Northing (m)
421	Pinus strobus	3	16.0	24.7	20	Mixed	112920	891478
422	Quercus sp.	2	21.1	47.5	20	Mixed	112909	891476
423	Tsuga canadensis	3	20.7	33.6	20	Mixed	112900	891477
424	Pinus strobus	2	35.8	54.3	20	Mixed	112875	891477
425	Quercus sp.	2	20.6	43.8	20	Mixed	112877	891491
426	Pinus strobus	1	38.4	63.2	20	Mixed	112882	891489
427	Quercus sp.	2	36.5	31.1	20	Mixed	112891	891492
428	Pinus strobus	2	29.3	30.2	20	Mixed	112918	891498
429	Quercus sp.	2	24.8	44.7	20	Mixed	112907	891496
430	Acer platanoides	4	12.5	13.3	20	Mixed	112896	891498
431	Pinus strobus	4	23.0	16.9	20	Mixed	112920	891520
432	Pinus strobus	4	12.9	20.3	20	Mixed	112908	891518
433	Acer platanoides	3	21.1	23.4	20	Mixed	112900	891521
434	Acer rubrum	3	15.3	12.7	20	Mixed	112878	891513
435	Pinus strobus	4	12.0	14.5	20	Mixed	112880	891533
436	Acer rubrum	4	14.7	14.4	20	Mixed	112888	891531
437	Acer platanoides	3	19.2	19.6	20	Mixed	112901	891532
487	Quercus sp.	1	33.3	49.3	19	Decid.	112991	891692
488	Quercus sp.	1	27.1	43.5	19	Decid.	113001	891693
489	Quercus alba	1	35.7	45.7	19	Decid.	113011	891689
490	Quercus sp.	2	24.5	36.1	19	Decid.	113020	891690
491	Quercus sp.	2	26.3	34.0	19	Decid.	113017	891671

Tag #	Species	Canopy	Height (m)	DBH (cm)	Plot	Forest type	Easting (m)	Northing (m)
492	Quercus sp.	2	30.6	41.9	19	Decid.	113003	891673
493	Quercus sp.	2	27.4	43.1	19	Decid.	112996	891674
494	Quercus sp.	2	27.8	32.7	19	Decid.	112988	891675
495	Quercus sp.	2	26.2	50.7	19	Decid.	112982	891675
496	Pinus strobus	4	12.0	12.8	19	Decid.	112964	891674
497	Quercus sp.	2	24.0	50.0	19	Decid.	112966	891656
498	Quercus sp.	3	28.4	24.2	19	Decid.	112971	891647
499	Quercus sp.	2	28.9	50.2	19	Decid.	112985	891637
500	Quercus sp.	2	34.7	34.2	19	Decid.	112993	891639
709	Quercus sp.	1	34.9	49.4	19	Decid.	112965	891634
710	Quercus sp.	3	14.9	20.2	19	Decid.	112979	891637
711	Acer rubrum	2	29.9	25.9	19	Decid.	112998	891656
712	Quercus sp.	1	33.5	53.4	19	Decid.	112991	891655
713	Acer rubrum	3	16.4	14.2	19	Decid.	112982	891693
714	Acer rubrum	4	12.4	12.1	19	Decid.	112973	891691
269	Betula lenta	2	14.9	15.6	18	Mixed	113117	891398
270	Pinus strobus	4	8.8	10.2	18	Mixed	113109	891398
271	Pinus strobus	2	10.5	21.0	18	Mixed	113098	891393
272	Betula lenta	2	12.4	18.9	18	Mixed	113088	891395
273	Pinus strobus	4	10.6	16.5	18	Mixed	113087	891373
274	Pinus strobus	2	10.9	18.8	18	Mixed	113099	891372
275	Betula lenta	2	12.5	16.3	18	Mixed	113109	891382
276	Pinus strobus	2	14.0	24.7	18	Mixed	113119	891382
277	Betula lenta	2	10.7	17.2	18	Mixed	113122	891361
278	Pinus strobus	4	10.0	12.2	18	Mixed	113113	891360
279	Betula lenta	2	16.2	19.4	18	Mixed	113098	891349
280	Pinus strobus	2	11.2	19.0	18	Mixed	113091	891354
281	Betula lenta	2	17.4	19.5	18	Mixed	113091	891336
282	Betula papyrifera	2	10.1	15.2	18	Mixed	113098	891333
283	Betula lenta	2	11.9	14.9	18	Mixed	113112	891342
284	Pinus strobus	2	13.8	22.3	18	Mixed	113122	891343
285	Pinus strobus	2	13.0	26.8	18	Mixed	113121	891325
286	Pinus strobus	2	12.6	25.2	18	Mixed	113111	891322
287	Betula lenta	2	11.9	13.0	18	Mixed	113099	891312
288	Betula papyrifera	2	16.7	16.4	18	Mixed	113090	891313
289	Betula papyrifera	2	16.2	23.5	18	Mixed	113093	891294

Tag #	Species	Canopy	Height (m)	DBH (cm)	Plot	Forest type	Easting (m)	Northing (m)
290	Betula papyrifera	2	14.3	13.0	18	Mixed	113099	891293
291	Pinus strobus	4	6.1	13.8	18	Mixed	113114	891300
292	Pinus strobus	2	12.8	27.2	18	Mixed	113123	891298
832	Acer saccharum	2	24.8	38.3	17	Decid.	113153	891648
833	Quercus sp.	2	29.7	34.7	17	Decid.	113152	891630
834	Quercus sp.	2	33.3	64.3	17	Decid.	113152	891610
835	Quercus sp.	2	25.9	27.4	17	Decid.	113156	891616
836	Quercus sp.	2	35.7	77.3	17	Decid.	113160	891611
837	Quercus sp.	2	25.7	49.6	17	Decid.	113166	891605
838	Betula lenta	2	27.1	30.1	17	Decid.	113167	891630
839	Quercus sp.	2	27.2	42.5	17	Decid.	113167	891645
840	Quercus sp.	1	32.9	51.3	17	Decid.	113161	891652
841	Tilia americana	2	28.4	39.4	17	Decid.	113160	891627
842	Quercus sp.	2	21.8	33.6	17	Decid.	113165	891634
241	Pinus strobus	4	20.6	25.8	16	Decid.	113070	891535
242	Pinus strobus	4	9.7	16.9	16	Decid.	113079	891534
243	Quercus sp.	4	13.2	13.1	16	Decid.	113092	891533
244	Carya sp.	1	35.0	75.1	16	Decid.	113101	891532
245	Betula lenta	2	28.7	30.4	16	Decid.	113099	891513
246	Betula lenta	4	17.7	22.5	16	Decid.	113092	891511
247	Quercus sp.	4	24.3	38.3	16	Decid.	113079	891514
248	Betula lenta	4	12.6	12.6	16	Decid.	113068	891515
249	Carya sp.	4	11.2	11.7	16	Decid.	113068	891497
250	Acer rubrum	4	13.8	14.4	16	Decid.	113080	891499
251	Acer saccharum	4	11.6	11.6	16	Decid.	113094	891497
252	Quercus sp.	2	17.9	37.6	16	Decid.	113103	891498
253	Betula lenta	2	33.3	41.6	15	Decid.	113103	891481
254	Acer rubrum	4	13.0	13.6	15	Decid.	113097	891479
255	Betula lenta	4	9.4	12.6	15	Decid.	113083	891473
256	Quercus sp.	2	26.3	33.1	15	Decid.	113074	891475
257	Acer rubrum	4	7.4	13.2	15	Decid.	113072	891458
258	Quercus sp.	2	24.5	29.0	15	Decid.	113083	891461
259	Pinus strobus	4	13.8	17.7	15	Decid.	113096	891464
260	Populus grandidentata	1	30.9	37.2	15	Decid.	113107	891461
262	Quercus sp.	2	24.2	44.1	15	Decid.	113108	891445

Tag #	Species	Canopy	Height (m)	DBH (cm)	Plot	Forest type	Easting (m)	Northing (m)
209	Quercus sp.	2	34.5	40.7	14	Decid.	113078	891702
210	Quercus sp.	1	42.4	62.8	14	Decid.	113084	891701
211	Betula lenta	4	18.0	14.0	14	Decid.	113090	891699
212	Betula lenta	4	26.4	20.9	14	Decid.	113103	891699
213	Betula lenta	2	22.5	23.7	14	Decid.	113101	891680
214	Betula lenta	4	21.5	17.6	14	Decid.	113092	891681
215	Betula lenta	4	19.2	14.3	14	Decid.	113085	891680
216	Quercus sp.	1	38.6	45.0	14	Decid.	113073	891681
217	Quercus sp.	1	31.2	40.2	14	Decid.	113076	891663
218	Quercus sp.	1	30.6	54.6	14	Decid.	113083	891655
219	Quercus sp.	1	29.6	52.9	14	Decid.	113093	891662
220	Betula lenta	4	18.4	20.2	14	Decid.	113098	891661
221	Betula lenta	2	19.5	19.5	14	Decid.	113101	891642
222	Quercus sp.	1	30.7	50.4	14	Decid.	113094	891642
223	Betula lenta	4	17.3	13.9	14	Decid.	113086	891639
224	Quercus sp.	2	28.8	32.9	14	Decid.	113080	891636
225	Quercus sp.	2	33.9	40.0	14	Decid.	113079	891616
226	Quercus sp.	2	34.2	33.4	14	Decid.	113090	891617
227	Quercus sp.	1	36.6	49.0	14	Decid.	113092	891620
228	Quercus sp.	2	23.1	38.4	14	Decid.	113098	891618
229	Quercus sp.	1	37.5	62.3	14	Decid.	113097	891597
230	Quercus sp.	3	23.1	23.7	14	Decid.	113092	891598
231	Quercus sp.	2	31.0	43.0	14	Decid.	113085	891594
232	Quercus sp.	1	34.4	63.3	14	Decid.	113074	891596
478	Quercus sp.	2	28.1	49.2	13	Decid.	112997	891734
479	Pinus strobus	4	8.8	12.3	13	Decid.	113006	891734
480	Acer platanoides	3	19.6	19.1	13	Decid.	113016	891737
484	Pinus strobus	3	12.3	16.5	13	Decid.	113012	891711
485	Quercus alba	2	19.8	24.9	13	Decid.	113001	891711
486	Populus deltoides	2	28.3	28.7	13	Decid.	112999	891715
715	Quercus sp.	2	32.5	30.2	13	Decid.	112977	891714
716	Quercus alba	2	19.4	27.9	13	Decid.	112988	891714
717	Quercus alba	3	22.0	26.2	13	Decid.	112988	891730
718	Acer rubrum	4	10.0	15.0	13	Decid.	112978	891731
701	Populus deltoides	2	29.3	27.0	12	Decid.	112992	891615
702	Quercus sp.	1	32.9	49.5	12	Decid.	112981	891615

Tag #	Species	Canopy	Height (m)	DBH (cm)	Plot	Forest type	Easting (m)	Northing (m)
703	Quercus sp.	2	21.5	26.8	12	Decid.	112973	891613
704	Quercus alba	2	28.5	30.8	12	Decid.	112962	891614
705	Quercus sp.	2	25.8	36.9	12	Decid.	112959	891595
706	Quercus sp.	2	30.3	54.8	12	Decid.	112972	891595
707	Quercus sp.	2	25.7	43.1	12	Decid.	112982	891590
708	Pinus strobus	3	19.8	29.6	12	Decid.	112990	891590
843	Quercus sp.	2	26.2	47.8	12	Decid.	112990	891574
844	Quercus sp.	2	21.0	35.1	12	Decid.	112982	891571
845	Quercus sp.	2	26.0	41.1	12	Decid.	112974	891572
201	Fagus grandifolia	2	16.0	26.0	11	Decid.	113082	891745
202	Quercus sp.	2	31.5	36.2	11	Decid.	113090	891744
203	Quercus sp.	2	29.3	45.7	11	Decid.	113100	891741
204	Betula lenta	4	17.6	19.5	11	Decid.	113108	891738
205	Acer rubrum	4	20.4	11.5	11	Decid.	113105	891722
206	Quercus sp.	4	15.6	13.9	11	Decid.	113099	891725
207	Quercus sp.	1	28.5	40.7	11	Decid.	113094	891722
208	Quercus sp.	2	18.6	25.4	11	Decid.	113081	891720
233	Quercus sp.	2	24.1	31.9	10	Decid.	113075	891577
234	Pinus strobus	4	14.5	12.5	10	Decid.	113084	891573
235	Carya sp.	4	26.1	16.8	10	Decid.	113090	891576
236	Betula lenta	2	29.7	27.5	10	Decid.	113096	891576
237	Quercus sp.	2	33.2	28.7	10	Decid.	113100	891556
238	Quercus sp.	1	35.2	42.0	10	Decid.	113093	891555
239	Quercus sp.	2	32.4	49.6	10	Decid.	113079	891558
240	Pinus strobus	4	16.4	20.1	10	Decid.	113072	891556
465	Quercus alba	2	26.6	33.3	9	Mixed	112922	891667
466	Quercus sp.	1	25.9	64.4	9	Mixed	112922	891688
467	Quercus sp.	1	27.5	49.5	9	Mixed	112912	891683
468	Pinus strobus	1	31.1	43.8	9	Mixed	112905	891685
469	Pinus resinosa	1	26.6	29.8	9	Mixed	112880	891674
470	Tsuga canadensis	2	27.4	55.6	9	Mixed	112883	891690
471	Pinus strobus	1	35.1	79.6	9	Mixed	112891	891689
472	Quercus sp.	2	17.8	22.0	9	Mixed	112902	891693
473	Acer rubrum	2	23.8	31.8	9	Mixed	112922	891703
474	Pinus strobus	4	20.5	20.2	9	Mixed	112920	891723
475	Pinus strobus	3	13.2	39.9	9	Mixed	112912	891722

Tag #	Species	Canopy	Height (m)	DBH (cm)	Plot	Forest type	Easting (m)	Northing (m)
476	Pinus strobus	1	30.8	66.5	9	Mixed	112903	891719
477	Pinus strobus	1	33.4	63.5	9	Mixed	112884	891711
12	Quercus sp.	2	21.8	13.1	8	Decid.	112910	891601
438	Quercus sp.	2	31.1	35.5	8	Decid.	112921	891542
439	Betula lenta	4	14.4	11.7	8	Decid.	112912	891538
440	Quercus sp.	2	33.3	70.0	8	Decid.	112900	891545
441	Quercus sp.	2	29.9	51.0	8	Decid.	112920	891563
442	Acer rubrum	3	20.6	19.3	8	Decid.	112914	891563
443	Pinus strobus	4	16.9	17.1	8	Decid.	112900	891563
444	Quercus sp.	2	23.3	35.1	8	Decid.	112880	891552
445	Quercus alba	2	21.5	41.5	8	Decid.	112877	891573
446	Acer platanoides	3	24.1	23.9	8	Decid.	112886	891571
447	Quercus sp.	2	37.0	55.0	8	Decid.	112897	891572
448	Pinus strobus	1	38.7	60.2	8	Decid.	112923	891583
449	Quercus sp.	3	16.7	19.2	8	Decid.	112923	891600
450	Betula lenta	2	19.9	26.6	8	Decid.	112922	891610
451	Populus grandidentata	2	29.5	41.8	8	Decid.	112913	891610
452	Quercus alba	4	14.4	19.5	8	Decid.	112879	891592
453	Betula lenta	4	9.4	11.9	8	Decid.	112870	891592
454	Betula lenta	3	16.6	14.5	8	Decid.	112878	891611
455	Quercus alba	2	24.9	31.5	8	Decid.	112891	891614
456	Populus grandidentata	2	21.2	31.3	8	Decid.	112902	891613
457	Quercus sp.	2	29.0	39.1	8	Decid.	112923	891618
459	Acer rubrum	3	14.7	16.3	8	Decid.	112910	891640
460	Quercus sp.	2	25.1	31.2	8	Decid.	112900	891639
461	Quercus alba	1	28.0	40.1	8	Decid.	112880	891634
462	Acer rubrum	4	11.3	13.6	8	Decid.	112881	891650
463	Quercus sp.	2	27.7	46.2	8	Decid.	112888	891652
464	Pinus strobus	4	9.0	14.0	8	Decid.	112897	891654
401	Quercus sp.	2	26.9	50.2	7	Decid.	112887	891376
402	Caryasp.	3	25.0	20.9	7	Decid.	112906	891379
403	Pinus strobus	1	39.3	66.2	7	Decid.	112918	891380
404	Quercus sp.	2	29.4	34.5	7	Decid.	112922	891397
405	Pinus strobus	1	35.2	45.8	7	Decid.	112914	891396
406	Pinus strobus	4	12.9	19.3	7	Decid.	112900	891400
407	Betula lenta	2	18.5	28.9	7	Decid.	112891	891395

Tag #	Species	Canopy	Height (m)	DBH (cm)	Plot	Forest type	Easting (m)	Northing (m)
408	Pinus strobus	3	18.3	23.7	7	Decid.	112879	891414
409	Pinus strobus	2	31.8	57.1	7	Decid.	112891	891417
410	Quercus sp.	1	38.2	63.8	7	Decid.	112910	891419
411	Pinus strobus	3	15.6	27.0	7	Decid.	112922	891418
412	Quercus sp.	2	35.2	35.6	7	Decid.	112924	891431
413	Quercus sp.	2	31.8	34.2	7	Decid.	112916	891436
414	Quercus sp.	1	32.4	62.0	7	Decid.	112907	891436
415	Betula lenta	4	16.3	11.9	7	Decid.	112894	891435
416	Quercus sp.	2	30.2	29.1	7	Decid.	112869	891429
417	Quercus sp.	2	22.5	23.5	7	Decid.	112874	891449
418	Quercus sp.	3	19.7	19.6	7	Decid.	112884	891449
419	Pinus strobus	4	11.9	17.1	7	Decid.	112896	891446
420	Quercus sp.	2	26.3	36.8	7	Decid.	112915	891457
361	Carya sp.	4	9.0	16.0	6	Decid.	112861	891176
362	Pinus strobus	4	15.8	16.6	6	Decid.	112870	891173
363	Pinus strobus	1	30.8	61.1	6	Decid.	112882	891171
364	Quercus sp.	2	22.3	38.4	6	Decid.	112883	891194
365	Pinus strobus	4	19.4	25.6	6	Decid.	112873	891193
366	Pinus strobus	4	18.6	26.2	6	Decid.	112865	891193
369	Pinus strobus	2	26.8	35.5	6	Decid.	112862	891211
370	Tsuga canadensis	4	12.9	43.5	6	Decid.	112870	891215
371	Pinus strobus	1	33.4	32.2	6	Decid.	112884	891218
372	Tsuga canadensis	4	6.8	10.1	6	Decid.	112884	891237
373	Quercus sp.	1	27.5	58.0	6	Decid.	112874	891236
374	Quercus alba	3	13.5	21.1	6	Decid.	112867	891236
377	Pinus strobus	4	11.9	12.7	6	Decid.	112868	891248
378	Quercus sp.	3	27.1	21.8	6	Decid.	112875	891250
379	Quercus sp.	2	21.0	36.4	6	Decid.	112892	891260
380	Pinus strobus	4	11.2	13.8	6	Decid.	112891	891281
381	Pinus strobus	3	16.4	19.3	6	Decid.	112883	891280
382	Quercus sp.	1	22.3	56.3	6	Decid.	112877	891283
383	Quercus sp.	1	21.2	57.3	6	Decid.	112860	891278
384	Quercus sp.	2	10.5	23.5	6	Decid.	112863	891296
385	Betula lenta	3	20.0	16.8	6	Decid.	112872	891293
386	Pinus strobus	4	13.2	11.8	6	Decid.	112880	891295
387	Quercus sp.	2	24.0	30.5	6	Decid.	112899	891302

Tag #	Species	Canopy	Height (m)	DBH (cm)	Plot	Forest type	Easting (m)	Northing (m)
388	Acer rubrum	2	25.9	17.4	6	Decid.	112901	891321
389	Pinus strobus	1	28.5	51.4	6	Decid.	112892	891318
390	Quercus sp.	2	24.0	35.0	6	Decid.	112884	891319
391	Quercus sp.	2	25.4	42.5	6	Decid.	112863	891315
392	Quercus sp.	2	17.5	29.7	6	Decid.	112868	891334
393	Quercus sp.	1	27.0	53.3	6	Decid.	112879	891335
394	Pinus strobus	1	34.1	44.3	6	Decid.	112889	891332
829	Quercus sp.	2	20.8	34.6	6	Decid.	112878	891160
830	Quercus sp.	2	18.8	43.7	6	Decid.	112870	891166
831	Quercus sp.	2	17.2	27.1	6	Decid.	112861	891162
100	Pinus rigida	2	18.2	44.4	5	Conifer	112770	891289
305	Quercus rubra	1	26.5	42.8	5	Conifer	112793	891305
306	Quercus rubra	2	14.2	23.0	5	Conifer	112785	891305
307	Pinus resinosa	2	25.5	25.7	5	Conifer	112776	891304
308	Pinus resinosa	2	20.0	23.0	5	Conifer	112768	891308
309	Pinus strobus	1	25.4	60.3	5	Conifer	112765	891339
310	Pinus resinosa	2	26.5	36.3	5	Conifer	112778	891332
311	Pinus resinosa	2	21.6	22.6	5	Conifer	112788	891331
312	Pinus resinosa	2	19.3	35.4	5	Conifer	112799	891322
313	Pinus resinosa	2	34.7	33.8	5	Conifer	112794	891342
314	Betula lenta	4	14.0	11.8	5	Conifer	112784	891342
315	Pinus resinosa	2	22.0	27.5	5	Conifer	112775	891342
316	Pinus strobus	1	30.3	62.0	5	Conifer	112768	891352
317	Pinus strobus	2	26.5	50.6	5	Conifer	112768	891370
318	Pinus strobus	2	33.1	62.8	5	Conifer	112779	891371
319	Pinus resinosa	2	34.2	39.0	5	Conifer	112787	891372
320	Pinus resinosa	2	23.7	21.7	5	Conifer	112795	891361
321	Pinus resinosa	2	31.4	30.5	5	Conifer	112797	891381
322	Pinus resinosa	2	28.5	31.4	5	Conifer	112787	891383
323	Pinus resinosa	2	23.5	28.0	5	Conifer	112778	891382
293	Pinus resinosa	2	20.5	21.5	4	Mixed	112768	891231
294	Quercus rubra	2	16.0	31.2	4	Mixed	112779	891231
295	Pinus resinosa	2	20.3	31.2	4	Mixed	112787	891231
296	Quercus rubra	2	20.9	37.6	4	Mixed	112795	891237
297	Pinus strobus	2	21.9	49.5	4	Mixed	112794	891259
298	Pinus rigida	2	19.7	31.0	4	Mixed	112783	891258
299	Quercus rubra	2	20.7	46.1	4	Mixed	112771	891258

Tag #	Species	Canopy	Height (m)	DBH (cm)	Plot	Forest type	Easting (m)	Northing (m)
300	Pinus resinosa	2	21.3	27.4	4	Mixed	112766	891247
301	Quercus rubra	2	31.0	48.3	4	Mixed	112762	891267
302	Quercus rubra	1	29.0	57.2	4	Mixed	112776	891270
303	Quercus rubra	2	19.0	23.3	4	Mixed	112785	891271
154	Pinus resinosa	2	32.5	40.3	3	Conifer	112796	891609
155	Pinus resinosa	2	26.7	32.0	3	Conifer	112784	891610
156	Pinus resinosa	2	22.8	32.7	3	Conifer	112775	891608
157	Pinus resinosa	2	25.1	31.2	3	Conifer	112762	891609
158	Pinus resinosa	2	33.8	36.1	3	Conifer	112799	891627
159	Pinus resinosa	2	22.0	26.9	3	Conifer	112787	891627
160	Pinus resinosa	2	24.6	24.9	3	Conifer	112775	891627
161	Pinus resinosa	0	30.0	22.1	3	Conifer	112766	891630
337	Pinus strobus	2	28.4	41.4	3	Conifer	112799	891464
338	Pinus resinosa	2	23.4	31.3	3	Conifer	112789	891465
339	Pinus strobus	2	32.8	70.8	3	Conifer	112778	891473
340	Pinus strobus	2	26.0	53.9	3	Conifer	112768	891481
341	Quercus rubra	4	13.9	36.1	3	Conifer	112770	891505
342	Pinus strobus	2	31.0	55.9	3	Conifer	112776	891507
343	Pinus strobus	2	30.5	36.3	3	Conifer	112788	891504
344	Pinus resinosa	2	20.8	20.4	3	Conifer	112797	891490
345	Pinus strobus	2	29.2	44.6	3	Conifer	112793	891511
346	Pinus strobus	2	30.0	46.2	3	Conifer	112784	891513
347	Pinus resinosa	2	21.8	19.1	3	Conifer	112770	891510
348	Tsuga canadensis	4	15.4	35.0	3	Conifer	112770	891534
349	Acer platanoides	4	14.4	10.1	3	Conifer	112768	891557
350	Pinus resinosa	2	26.8	29.7	3	Conifer	112778	891563
351	Pinus strobus	1	29.6	82.9	3	Conifer	112790	891557
352	Pinus strobus	2	30.4	43.3	3	Conifer	112788	891527
353	Pinus strobus	4	18.8	21.0	3	Conifer	112793	891553
354	Pinus strobus	2	30.3	67.6	3	Conifer	112782	891548
355	Pinus resinosa	2	28.2	41.4	3	Conifer	112770	891549
356	Pinus resinosa	2	27.3	35.2	3	Conifer	112769	891587
357	Pinus resinosa	2	25.8	22.9	3	Conifer	112777	891585
358	Acer rubrum	2	24.9	55.2	3	Conifer	112795	891579
359	Pinus resinosa	2	23.6	28.2	3	Conifer	112786	891595
324	Pinus resinosa	2	27.5	21.5	2	Conifer	112769	891393

Tag #	Species	Canopy	Height (m)	DBH (cm)	Plot	Forest type	Easting (m)	Northing (m)
325	Pinus strobus	2	32.8	55.8	2	Conifer	112772	891413
326	Pinus resinosa	2	29.2	33.2	2	Conifer	112782	891415
327	Pinus resinosa	2	33.0	31.5	2	Conifer	112793	891411
328	Pinus resinosa	2	32.6	27.0	2	Conifer	112804	891405
329	Pinus strobus	1	54.0	92.1	2	Conifer	112798	891423
330	Pinus resinosa	2	21.9	33.3	2	Conifer	112782	891423
331	Pinus strobus	1	38.0	68.9	2	Conifer	112781	891429
332	Pinus resinosa	2	33.2	32.2	2	Conifer	112768	891435
333	Pinus resinosa	2	29.7	37.4	2	Conifer	112765	891459
334	Pinus resinosa	2	16.4	25.9	2	Conifer	112780	891457
335	Pinus resinosa	2	20.7	37.7	2	Conifer	112791	891456
336	Pinus resinosa	2	23.4	36.9	2	Conifer	112799	891446
162	Acer platanoides	3	16.3	12.5	1	Conifer	112802	891652
163	Pinus resinosa	2	19.4	30.8	1	Conifer	112785	891655
164	Acer platanoides	2	18.1	39.1	1	Conifer	112780	891654
165	Pinus resinosa	2	21.0	37.2	1	Conifer	112773	891658
166	Pinus resinosa	0	19.5	25.9	1	Conifer	112803	891669
167	Betula lenta	0	10.4	10.4	1	Conifer	112792	891671
168	Pinus resinosa	0	27.3	32.3	1	Conifer	112781	891671
169	Acer platanoides	0	15.5	12.1	1	Conifer	112771	891674
170	Pinus resinosa	0	19.2	33.1	NA	NA	112805	891689
171	Pinus resinosa	0	23.2	22.5	NA	NA	112796	891689
172	Pinus resinosa	0	27.0	37.8	NA	NA	112785	891691
173	Pinus resinosa	0	24.3	27.4	NA	NA	112773	891697
174	Pinus resinosa	0	25.4	35.7	NA	NA	112808	891719
175	Pinus resinosa	0	20.5	36.8	NA	NA	112797	891718
176	Pinus resinosa	0	25.0	37.5	NA	NA	112788	891717
177	Pinus resinosa	0	18.5	35.9	NA	NA	112778	891715
261	Acer rubrum	1	31.0	65.3	NA	NA	113116	891439
263	Quercus sp.	1	27.3	70.4	NA	NA	113098	891434
264	Acer rubrum	4	19.9	20.6	NA	NA	113086	891434
265	Carya sp.	1	31.6	35.9	NA	NA	113088	891416
266	Quercus sp.	1	26.3	40.9	NA	NA	113096	891416
267	Acer rubrum	4	17.0	25.4	NA	NA	113109	891420
268	Sassafras albidum	4	16.3	27.0	NA	NA	113113	891420

Tag #	Species	Canopy	Height (m)	DBH (cm)	Plot	Forest type	Easting (m)	Northing (m)
304	Pinus rigida	2	17.8	26.1	NA	NA	112793	891284
360	Quercus alba	4	29.2	32.8	NA	NA	112854	891173
367	Quercus alba	2	21.9	29.5	NA	NA	112850	891194
368	Quercus alba	1	21.1	40.1	NA	NA	112851	891210
375	Quercus sp.	2	32.4	45.5	NA	NA	112854	891233
376	Carya sp.	4	18.2	15.5	NA	NA	112857	891252
395	Acer rubrum	4	20.0	17.3	NA	NA	112904	891340
396	Pinus strobus	4	18.6	19.6	NA	NA	112915	891359
397	Acer rubrum	3	18.6	14.3	NA	NA	112904	891358
398	Acer rubrum	4	19.8	12.9	NA	NA	112893	891358
399	Acer platanoides	3	22.5	15.4	NA	NA	112888	891360
400	Acer rubrum	3	23.1	17.8	NA	NA	112881	891371
458	Acer rubrum	3	13.3	12.7	NA	NA	112924	891639
481	Quercus sp.	3	12.0	16.6	NA	NA	113025	891738
482	Pinus strobus	3	20.1	24.5	NA	NA	113029	891736
483	Pinus strobus	4	16.6	16.8	NA	NA	113022	891713
824	Quercus sp.	2	21.1	47.8	NA	NA	112852	891160
825	Quercus sp.	1	16.5	47.8	NA	NA	112845	891148
826	Quercus sp.	2	23.6	61.0	NA	NA	112862	891143
827	Quercus sp.	2	21.6	37.3	NA	NA	112872	891149
828	Quercus sp.	2	18.8	36.9	NA	NA	112877	891143

Appendix 2. Coordinates of the Southeast corner of each plot (height analysis) and subplot (biomass analysis). Coordinates are Massachusetts State Plane Coordinate System, mainland NAD 1983.

Plot number	Subplot number	Easting (m)	Northing (m)
1		112749	891650
2		112749	891388
3		112751	891464
4		112740	891228
5		112748	891289
6		112858	891158
7		112861	891372
8		112862	891537
9		112860	891665
10		113063	891551
11		113057	891714
12		112955	891562
13		112962	891701
14		113060	891592
15		113063	891440
16		113063	891483
17		113143	891604
18		113070	891292
19		112961	891626
20		112860	891470
	2.2	112769	891521
	3.0	112860	891146
	5.0	113079	891708
	230.0	113062	891597
	236.0	113067	891547
	272.0	113087	891365
	311.0	112759	891302
	388.0	112871	891292
	428.0	112888	891498
	486.0	112968	891685
	499.0	112956	891636

Appendix 3. Species-specific biomass equations from Jenkins et al. 2004 and a mixed hardwood equation from Jenkins et al. 2003.

Species	Max DBH (cm)	Study sample size	Biomass equation	Study location
Aspen, Big Tooth	33.8	30	=(((EXP(-2.32+0*DBH+2.377*(LN(DBH^1))))*0.001*1.01)	Nova Scotia
Beech, American	63.0	14	=(10^(2.111+2.462*(LOG((DBH^1),10))))*0.000001	Hubbard Brook, NH
Birch, Black	39.6	10	=((10^(-1.248+2.726*(LOG((DBH^1),10))))*0.001)*1.016	Southern Appalachian
Birch, Paper	32.8	45	=((EXP(-2.231+0*DBH+2.431*(LN(DBH^1))))*0.001)*1.01	Nova Scotia
Hemlock, Eastern	55.0	31	=(EXP(0.68+0*DBH+2.362*(LN(DBH^1))))*0.00045359237	Maine
Hickory, spp.	52.3	10	=((10^(-1.326+2.762*(LOG(DBH^1))))*0.001)*1.005	Southern Appalachian
Maple, Norway	42.0	x	=(EXP(-1.51+0*DBH+2.1*(LN(DBH^1))))*0.001	Refit from UT FIA data-bigtooth maple
Maple, Red	52.2	150	=((EXP(-1.721+0*DBH+2.334*(LN(DBH^1))))*0.001)*1.007	x
Maple, Sugar	69.5	18	=((EXP(-2.192+0.011*DBH+2.67*(LN(DBH^1))))*0.001)*1.059	Wisconsin
Oak, Red	69.5	16	=((EXP(-2.972+0.017*DBH+2.873*(LN(DBH^1))))*0.001)*1.05	Wisconsin
Oak, White	63.0	10	=((10^(-1.266+2.613*(LOG((DBH^1),10))))*0.001)*1.024	Southern Appalachian
Pine, Red	34.3	47	=((EXP(-2.468+0*DBH+2.35*(LN(DBH^1))))*0.001)*1.01	Nova Scotia
Pine, White	55.0	x	=(EXP(5.283+0*DBH+2.037*(LN(DBH^1))))*0.000001	Northeast
Pine, Pitch	31.0	15	=(10^2.017+2.337*(LOG((DBH^1),10)))*0.000001	New York
Mixed Hardwood	unknown	289	=(EXP(-2.48+2.4835*LN(DBH)))*0.001	United States

Appendix 4. Data and methodology for estimation of biomass using remote data. Line 2 shows the equations used to calculate the first line in the spreadsheet. Letters correspond to column, with the first column, plot, being column A. The methodology remains constant but the regression equations change to reflect species present.

plot	lidar height (actual)	height (predicted from lidar)	species	# trees/ spp	total stems/ 30x30	image stems/ha	trees/ spp/ ha	reg lnDBH	DBH	biomass	spp. total biomass	total plot biomass
		=0.511+(1.096*lidar)			=SUM(E$4:E$9)	=10000*(F2/900)	=10000*(E2/900)	=2.192+(0.055*C2)	=EXP(I2)	=(EXP(5.283+0*J2+2.037*(LN(J2^1))))*0.000001	=H2*K2	
428	24.868	27.766	wp	1	27.0	300.0	11.1	3.719118	41.22801	0.384171045	4.268567	
428	24.868	27.766	bb	3	27.0	300.0	33.3	3.276163	26.47399	0.43400968	14.46699	
428	24.868	27.766	ro	15	27.0	300.0	166.7	3.699739	40.43676	1.117350986	186.2252	
428	24.868	27.766	rm	3	27.0	300.0	33.3	3.390586	29.68335	0.483023918	16.1008	
428	24.868	27.766	mh	6	27.0	300.0	66.7	3.504649	33.26978	0.504615591	33.64104	
428	24.868	27.766	wo	0	27.0	300.0	0.0	3.574505	35.67695	0.631959468	0	254.7
2.2	26.953	30.051	wp	31	35.0	388.9	344.4	3.844802	46.74941	0.496262879	170.935	
2.2	26.953	30.051	hem	3	35.0	388.9	33.3	4.27726	72.04278	2.417672527	80.58908	
2.2	26.953	30.051	mh	1	35.0	388.9	11.1	3.634904	37.8982	0.697346935	7.748299	259.3
						388.9						
486	23.379	26.134	bb	2	24.0	266.7	22.2	3.20763	24.72044	0.360051617	8.001147	
486	23.379	26.134	ro	7	24.0	266.7	77.8	3.649156	38.4422	0.999542016	77.74216	
486	23.379	26.134	sm	1	24.0	266.7	11.1	3.395569	29.83161	0.737558756	8.195097	
486	23.379	26.134	mh	0	24.0	266.7	0.0	3.411641	30.31495	0.400538859	0	
486	23.379	26.134	wo	1	24.0	266.7	11.1	3.52229	33.86188	0.551359451	6.126216	

plot	lidar height (actual)	height (predicted from lidar)	species	# trees/ spp	total stems/ 30x30	image stems/ha	trees/ spp/ ha	reg lnDBH	DBH	biomass	spp. total biomass	total plot biomass
486	23.379	26.134	hi	3	24.0	266.7	33.3	3.410248	30.27276	0.584563703	19.48546	
486	23.379	26.134	bta	10	24.0	266.7	111.1	3.395569	29.83161	0.317734822	35.30387	162.6
5	25.106	28.028	bb	4	27.0	300.0	44.4	3.287155	26.76661	0.447211766	19.87608	
5	25.106	28.028	ro	18	27.0	300.0	200.0	3.707853	40.76617	1.137315432	227.4631	
5	25.106	28.028	rm	2	27.0	300.0	22.2	3.404458	30.09797	0.498890468	11.08645	
5	25.106	28.028	mh	2	27.0	300.0	22.2	3.519568	33.76983	0.523662067	11.63693	
5	25.110	28.032	bta	1	27.0	300.0	11.1	3.488546	32.73833	0.396321289	4.40357	274.5
						300.0						
230	24.389	27.241	wp	1	25.0	277.8	11.1	3.690256	40.05509	0.362235973	4.024844	
230	24.389	27.241	ro	14	25.0	277.8	155.6	3.683471	39.78426	1.078224735	167.7238	
230	24.389	27.241	mh	4	25.0	277.8	44.4	3.474738	32.28936	0.46848847	20.82171	
230	24.389	27.241	wo	2	25.0	277.8	22.2	3.557712	35.08285	0.604829455	13.44065	
230	24.389	27.241	rm	2	25.0	277.8	22.2	3.362774	28.86916	0.452715081	10.06034	
230	24.389	27.241	bb	2	25.0	277.8	22.2	3.254123	25.89688	0.408701665	9.082259	225.2
3	21.479	24.052	wp	0	25.0	277.8	0.0	3.514844	33.61068	0.25340322	0	
3	21.479	24.052	ro	13	25.0	277.8	144.4	3.584603	36.03905	0.864966478	124.9396	
3	21.479	24.052	rm	4	25.0	277.8	44.4	3.193741	24.37945	0.305336847	13.57053	
3	21.479	24.052	mh	6	25.0	277.8	66.7	3.292947	26.9221	0.298280687	19.88538	

plot	lidar height (actual)	height (predicted from lidar)	species	# trees/ spp	total stems/ 30x30	image stems/ha	trees/ spp/ ha	reg lnDBH	Dbh	biomass	spp. total biomass	total plot biomass
3	21.479	24.052	wo	2	25.0	277.8	22.2	3.455655	31.67902	0.463251232	10.29447	168.7
272	12.510	14.222	wp	48	77.0	855.6	533.3	2.974208	19.57411	0.084243045	44.92962	
272	12.510	14.222	ro	0	77.0	855.6	0.0	3.279881	26.5726	0.423330552	0	
272	12.510	14.222	mh	20	77.0	855.6	222.2	2.732652	15.3736	0.07418341	16.4852	
272	12.510	14.222	wo	0	77.0	855.6	0.0	3.141103	23.12936	0.203638264	0	
272	12.510	14.222	rm	0	77.0	855.6	0.0	2.672764	14.47993	0.090698411	0	
272	12.510	14.222	bb	9	77.0	855.6	100.0	2.707322	14.98909	0.092056986	9.205699	70.62
236	26.797	29.880	wp	0	24.0	266.7	0.0	3.83541	46.31242	0.48685924	0	
236	26.797	29.880	ro	20	24.0	266.7	222.2	3.765286	43.17604	1.287507251	286.1127	
236	26.797	29.880	mh	3	24.0	266.7	33.3	3.62517	37.53112	0.680692589	22.68975	
236	26.797	29.880	wo	0	24.0	266.7	0.0	3.642166	38.17443	0.754174065	0	
236	26.797	29.880	rm	0	24.0	266.7	0.0	3.50265	33.20331	0.627142522	0	
236	26.797	29.880	bb	1	24.0	266.7	11.1	3.364968	28.93256	0.552884483	6.143161	314.9
499	28.017	31.218	wp	0	24.0	266.7	0.0	3.90897	49.84757	0.565559848	0	
499	28.017	31.218	ro	20	24.0	266.7	222.2	3.806747	45.00378	1.406006622	312.4459	
499	28.017	31.218	mh	1	24.0	266.7	11.1	3.701405	40.50417	0.822574764	9.13972	
499	28.017	31.218	wo	0	24.0	266.7	0.0	3.684964	39.8437	0.843411787	0	
499	28.017	31.218	rm	1	24.0	266.7	11.1	3.573534	35.64235	0.739767077	8.219634	

plot	lidar height (actual)	height (predicted from lidar)	species	# trees/ spp	total stems/ 30x30	image stems/ha	trees/ spp/ ha	reg lnDBH	Dbh	biomass	spp. total biomass	total plot biomass
499	28.017	31.218	bb	2	24.0	266.7	22.2	3.421141	30.6043	0.64437205	14.31938	344.1
388	22.324	24.979	wp	7	24.0	266.7	77.8	3.56582	35.36844	0.281130709	21.86572	
388	22.324	24.979	ro	8	24.0	266.7	88.9	3.613335	37.08953	0.922769077	82.02392	
388	22.324	24.979	mh	9	24.0	266.7	100.0	3.345777	28.38262	0.340099075	34.00991	
388	22.324	24.979	wo	0	24.0	266.7	0.0	3.485313	32.63265	0.500580087	0	
388	22.324	24.979	rm	0	24.0	266.7	0.0	3.242863	25.60692	0.342362529	0	
388	22.324	24.979	bb	0	24.0	266.7	0.0	3.159099	23.54936	0.315434303	0	137.9

WORKS CITED

Andersson, K., T.P. Evans, and K.R. Richards. 2009. Methods and approaches to national forest carbon inventories. Online supplement to: National forest carbon inventories: policy needs and assessment capacity. Climatic Change 93:69-101. Available from www.sobek.colorado.edu/~anderssk/KA_TE_KR_CC_supplement.pdf (accessed July 2011).

Archer D. 2005. Fate of fossil fuel CO_2 in geologic time. Journal of Geophysical Research 110:C09S05.

Avery, T.E. and H.E. Burkart. 1993. Forest Measurements 4th Ed. McGraw-Hill, Boston, MA.

Berg, L. 2008. Introductory botany: plants, people, and the environment. Thomson Brooks/Cole US.

Birdsey, R.A. 1992. Carbon storage and accumulation in the United States forest ecosystems. USDA (United States Department of Agriculture) Forest Service GenTech Report WO-59.

Bonner, G.M. 1964. A tree volume table for red pine by crown width and height. The Forestry Chronicle 40(3):339-346.

Boudreau, J., R.F. Nelson, H.A. Margolis. 2008. Regional aboveground forest biomass using airborne and spaceborne LiDAR in Quebec. Remote Sensing of Environment 112(10):3876-3890.

Brown, S. 2002. Measuring carbon in forests: current status and future challenges. Environmental Pollution 116:363-372.

Brown, S.L. and P.E. Schroeder. 1999. Spatial patterns of aboveground production and mortality of woody biomass for Eastern U.S. forests. Ecological Applications 9(3):968-980.

Brown, S., P. Schroeder, and R. Birdsey. 1997. Aboveground biomass distribution of US eastern hardwood forests and the use of large trees as an indicator of forest development. Forest Ecology and Management 96:37-47.

Cook B., R. Dubayah, F. Hall, R. Nelson, J. Ranson, A. Strahler, P. Siqueira, M. Simard, and P. Griffith. 2011. NACP New England and Sierra National Forests Biophysical Measurements: 2008-2010. Oak Ridge National Laboratory Distributed Active Archive Center, Oak Ridge, Tennessee, U.S.A. Available from http://dx.doi.org/10.3334/ORNLDAAC/1046 (accessed February 2012). .

Crone, E.E. and J. L. Gehring. 1997. Population viability of *Rorippa columbiae*: multiple models and spatial trend data. Conservation Biology 12(5):1054-1065.

Denny, E. and T. Siccama. 2001. How do we quantify a forest? Hubbard Brook Ecosystem Study. NH. Available from http://www.hubbardbrook.org/w6_tour/biomass-stop/how-to-quantify.htm#fhteqn (accessed July 2011).

FAO (Food and Agricultural Organization of the United Nations). 2011. State of the world's forests. Rome, Italy. Available from www.fao.org (accessed on March 2012).

Foster, D.R., G. Motzkin, and B. Slater. 1998. Land-use history as long-term broad-scale disturbance: regional forest dynamics in central New England. Ecosystems 1:96-119.

Gaveau, D.L.A and R.A. Hill. 2003. Quantifying canopy height underestimation by laser pulse penetration in small-footprint airborne laser scanning data. Canadian Journal of Remote Sensing 29(5):650-675.

Gower, S.T., R.E. McMurtrie, and D. Murty. 1996. Aboveground net primary production decline with stand age: potential causes. Trends in Evolution and Ecology 11(9):378-382.

Groom, M.J., G.K. Meffe, and C.R. Carroll. 2006. Principles of conservation biology. Sinauer Associates, Inc. Sunderland, MA.

Harding, D.J. 2000. Principles of airborne laser altimeter terrain mapping. NASA's Goddard Space Flight Center, Greenbelt, MD.

Hershey, R.R. and W.A. Befort. 1995. Aerial photo guide to New England forest cover types. United States Department of Agriculture Forest Service General Technical Report NE-195.

Houghton, J. 2005. Global warming. Reports on Progress in Physics 68-1343-1403.

Houghton, R.A. 2005. Aboveground forest biomass and the global carbon balance. Global Change Biology 11:945-958.

Hughes, L.H. 2000. Biological consequences of global warming: is the signal already. Trends in Ecology and Evolution 15(2):56-60.

IPCC (Intergovernmental Panel Climate Change). 2000. Good practice guidance and uncertainty management in national greenhouse gas inventories LULUCF (Land use, Land Use Change, and Forestry). IPCC Task Force on National Greenhouse Gas Inventories.

IPCC (Intergovernmental Panel Climate Change). 2007. Summary for policymakers. In: Climate Change 2007: The physical science basis. Contribution of working group I to the Fourth Assessment Report of the Intergovernmental Panel on Climate Change [Solomon, S., D. Qin, M. Manning, Z. Chen, M. Marquis, K.B. Averyt, M. Tignor and H.L. Miller (eds.)]. Cambridge University Press, Cambridge, United Kingdom and New York, NY, USA.

Jenkins, J.C., D.C. Chojnacky, L.S. Heath, and R.A. Birdsey. 2004. Comprehensive database of diameter-based biomass regressions for North American tree species. USDA Forest Service Northeastern Research Station General Technical Report NE-319.

Jenkins, J.C., D.C. Chojnacky, L.S. Heath, and R.A. Birdsey. 2003. National-scale biomass estimators for United States tree species. Forest Science 49(1):12-34.

Jenkins, J.C., Birdsey, R.A., and Y. Pan. 2001. Biomass and NPP estimation for the mid-Atlantic region (USA) using plot-level forest inventory data. Ecological Applications 1(4):1174-1193.

Keeling, C.D. 1973. Industrial production of carbon dioxide from fossil fuels and limestone. Tellus 25(2):174-198.

Lamson, N.I. 1987. D.b.h./crown diameter relationships in mixed Appalachian hardwood stands. United States Department of Agriculture Forest Service. Research Paper NE-610.

Leftsky, M.A., W.B. Cohen, G.G. Parker, and D.J. Harding. 2002. Lidar remote sensing for ecosystem studies. BioScience 52(1):19-30.

Lu, J. and L. Zhang. 2012. Geographically local linear mixed models for tree height diameter relationship. Forest Science 58:75-84.

Malhi, Y., P. Meir, S. Brown. 2002. Forests, carbon and global climate. The Royal Society 360(1797):1567-1591.

MassGIS. 2010. Soils_polygon. NRCS (National Resources Conservation Service) SSURGO (Soil Survey Geographic)-Certified Soils layer. Office of Geographic Information (MassGIS)/ Commonwealth of Massachusetts Information Technology Division. Available from www.mass.gov/mgis (accessed December 2010).

McKinley, D.C., M.G. Ryan, R.A. Birdsey, C.P. Giardina, M.E. Harmon, L.S. Heath, R.A. Houghton, B.B. Jackson, J.F. Morrison, B.C. Murray, D.E. Pataki, and K. E. Skog. 2011. A synthesis of current knowledge on forests and carbon storage in the United States. Ecological Applications 21(6):1902-1924.

Meyer, K.A. 2011. Determining allometric relationships within tree species for a quantitative understanding of atmosphere water fluxes coupled with remote-sensing based methods for determining forest structure at an individual-tree scale. Honors Research with Distinction Thesis. Ohio State University, OH. Available from http://hdl.handle.net/1811/48759 (accessed December 2011).

MFLA (Massachusetts Forests Landowners Association). No date. Common forest types in Massachusetts. Available from http://www.massforests.org/ma-forests/common-types.htm (accessed 11/11).

Miles P.D. and W.B. Smith. 2009. Specific gravity and other properties of wood and bark for 156 tree species found in North America. United States Department of Agriculture Forest Service Northern Research Station PA Research Note NRS-38.

Millette and Hayward. 2005. Detailed forest stand metrics taken from AIMS-1 sensor data. ASPRS Annual Conference. Baltimore, MD.

Mitchell, A. 2005. The ESRI guide to GIS analysis: Volume 2: spatial measurements and statistics. ESRI Press, Redlands, CA.

NCFMP (North Carolina Floodplain Mapping Program). 2003. Lidar and Digital Elevation Data. Available from http://www.ncfloodmaps.com/pubdocs/lidar_final_jan03.pdf (accessed 12/2011).

Nelson, R., R. Oderwald, and T.G. Gregoire. 1997. Separating the ground and airborne laser sampling phases to estimate tropical forest basal area, volume, and biomass. Remote Sensing Environment 60:311-236.

Nelson, R., M.A. Valenti, A. Short, and C. Keller. 2003. A Multiple resource inventory of Delaware using airborne laser data. BioScience 53(10):981-991.

Olson, J.S., J.A. Watts, L.J. Allison. 1985. Major world ecosystem complexes ranked by carbon in live vegetation: a database. ORNL NDP-017.

Pan, Y., R.A. Birdsey, J. Fang, R. Houghton, P.E. Kauppi, W.A. Kurz, O.L. Phillips, A. Shvidenko, S.L. Lewis, J.G. Canadell, P. Ciais, r.B. Jackson, S.W. Pacala, A.D. McGuire, S. Piao, a. Rautiainen, S. Sitch, D. Hayes. 2011. A large and persistent carbon sink in the world's forests. Science 333:988-993.

Patenaude, G., R.A. Hill, R. Milne, D.L.A. Gaveau, B.B.J. Briggs, and T.P. Dawson. 2004. Quantifying forest aboveground carbon content using lidar remote sensing. Remote Sensing of Environment 93:368-380.

Popescu, S.C. 2007. Estimating biomass of individual pine trees using airborne lidar. Biomass and Bioenergy 31:646-655.

Popescu S. C., R. H. Wynne, and J. A. Scrivani. 2004. Fusion of small-footprint lidar and multispectral data to estimate plot-level volume and biomass in deciduous and pine forests in Virginia, USA. Forest Science 50:551-565.

Popescu, S.C., K. Zhao, A. Neuenschwander, and C. Lin. 2011. Satellite lidar vs. Small footprint airborne lidar: comparing the accuracy of aboveground biomass estimates and forest structure metrics at footprint level. Remote Sensing of Environment 115:2786-2797.

Sayn-Wittgenstein, L. 1978. Recognition of tree species on aerial photographs. Canadian Forestry Service Division of the Environment Info Report FMR-X-118.

Schlesinger, W.H. 1997. Biogeochemistry: An analysis of global change. Academic Press, New York.

Sharma, M. and J. Parton. 2007. Height-diameter equations for boreal tree species in Ontario using a mixed-effects modeling approach. Forest Ecology and Management 249:187-198.

Swain, P.C. and J.B. Kearsley. 2001. Classification of the natural communities of Massachusetts. Natural Heritage & Endangered species Program Massachusetts Division of Fisheries and Wildlife, Westborough, MA. Ver.1.3, draft.

Tang, G., B. Beckage, B. Smith, and P.A. Miller. 2010. Estimating potential forest NPP, biomass and their climatic sensitivity in New England using a dynamic ecosystem model. Ecosphere ESA Journals 1:1-20.

USDA (United States Department of Agriculture) Forest Service. 2010. Live aboveground carbon storage in U.S. forests, by state, sub-region, and ownership group. Forest Inventory Data Online (FIDO). Available from www.fia.fs.fed.us (accessed January 2012).

US EPA (United States Environmental Protection Agency). 2012. Level III ecoregions. Western Ecology Division. Available from www.epa.gov/wed/pages/ecoregions.htm (accessed on January 2012).

USGS (United States Geological Survey). 1979. Mt. Holyoke quadrangle Massachusetts. Denver, CO.

Whittaker R.H. and G.M. Woodwell. 1967. Surface area relations of woody plants and forest communities. American Journal of Botany 54(8):931-939.

Zhao, K. S. Popescu, X. Meng, Y. Pang, and M. Agca. 2011. Characterizing forest canopy structure with lidar composite metrics and machine learning. Remote Sensing of Environment 115:1978-1996.

Zhang, L. B. Huiquan, P. Cheng, and C.J. Davis. 2003. Modeling spatial variation in tree diameter-height relationships. Forest Ecology and Management 189:317-329.